Bulletin of Engineering Geology and the Environment (2026) 85:363
https://doi.org/10.1007/s10064-026-05022-x

ORIGINAL PAPER

Evaluating completeness and consistency in earthquake-induced ground effects inventorying: insights from the last release of the Italian CEDIT catalogue

Matteo Fiorucci[1,2] · **Gian Marco Marmoni**[3] · **Federico Feliziani**[3] · **Salvatore Martino**[3]

Received: 19 September 2025 / Accepted: 2 May 2026

Abstract
The completeness and consistency of ground effect catalogues are critical for reliable analysis of scenarios in a multi-hazard risk perspective under a multidisciplinary framework, particularly for assessing the impact of earthquake-induced landslides on the environment and human activities. The updated Italian Catalogue of Earthquake-Induced Ground Failures - CEDIT (http://gdb.ceri.uniroma1.it) addresses these issues by integrating historical and recent data. This release expands the 2014 version by including seismic events up to the 2022 Adriatic coast and the 2025 Campi Flegrei earthquakes, and revisions based on recent publications and reports. It currently documents 4256 earthquake-induced ground effects, landslides, ground cracks, liquefactions, surface faulting, and ground changes, triggered by 215 events since 1117 A.D. Using this compilation, the paper provides an operational appraisal of catalogue completeness and spatial coverage, highlighting key sources of bias (e.g., overlapping effects during multi-event sequences) and identifying survey gaps through GIS-based visibility diagnostics, and updates the Italy-calibrated magnitude-maximum distance relationship for disrupted landslides, which offers an empirically constrained first-order tool for scenario delineation. Despite intrinsic limitations arising from heterogeneous historical reporting and the under representation of low-magnitude events, the extended spatio-temporal coverage of CEDIT supports reproducible national-to-regional analyses, improves comparisons across occurred scenarios of earthquake-induced effects, and provides actionable constraints for susceptibility modelling and risk-management applications in complex seismotectonic contexts.

Keywords Earthquake-induced ground effects · Landslides · Scenario analysis · Seismic hazard · CEDIT catalogue

Introduction

Damages caused by earthquakes are commonly linked to dramatic losses of life and buildings. Nevertheless, the environment can also experience deep changes as an aftermath of strong motions, through the occurrence of ground effects like landslides, ground cracks, surface faulting, environmental changes, and soil liquefaction, which can be more impactful than the ground shaking (Bird and Bommer 2004; Velázquez-Bucio et al. 2024). Such a chain effect intensifies the severity of the seismic hazard in a "domino-like" scenario, which can be regarded from a multi-hazard perspective (Fan et al. 2019 and references therein).

For seismic events, the availability of long-term earthquake catalogues (e.g., Guidoboni et al. 2018, 2019; Rovida et al. 2020a, b) are crucial for risk assessment (Stucchi et al. 2011), given the strong aperiodicity of the recurrence interval. To ensure reliability, these catalogues must draw from both documentary and historical reconstructions based on chronicles and pictorial representations that detail macroseismic intensity distribution (Locati et al. 2022). Such sources provide valuable information about the temporal

✉ Gian Marco Marmoni
gianmarco.marmoni@uniroma1.it

[1] Department of Civil and Mechanical Engineering, University of Cassino and Southern Lazio, Via G. Di Biasio 43, Cassino, FR I-03043, Italy

[2] European University of Technology, European Union EUt+, Cassino, FR, Italy

[3] Department of Earth Sciences and CERI Research Centre on Geological Risks, University of Rome "Sapienza", P.le Aldo Moro 5, Rome I-00185, Italy

Published online: 14 May 2026

occurrence and epicentral and hypocentral locations (Sbarra et al. 2019). For ground effects, studies that have analyzed past landslide scenarios, i.e., specifically the evaluation of the distribution of irreversible modifications induced by historical earthquakes, can help to infer the location and intensity or magnitudes of paleo-earthquakes (Rasanen and Maurer 2022 ; Pizza et al. 2024). This can be achieved through geological surveying and trigger modelling, which account for earthquake magnitude and local shaking intensity; this last one is efficient with respect to the induced ground effects (Crozier 1992; Jibson 1996; Clague 2022).

Engineering geology deals with earthquake-induced ground effects with particular attention to the landslides, projected towards the reconstruction of landslides distribution (Harp et al. 2011), by collecting surveyed data within catalogues (Govi 1977; Harp et al. 1981; Harp and Keefer 1990; Harp and Jibson 1995, 1996; Wills and McCrink 2002; Yagi et al. 2009; Comerci et al. 2015; Tang et al. 2016; Tanyaş et al. 2019), which are featured by their level of completeness, precision and reliability (Tanyas and Lombardo 2020). Due to the recent advancements in remote sensing, acquiring images covering large areas is now possible. This improvement enhances the coverage and completeness of inventories of effects collected after earthquake events (Harp et al. 2011).

The seismic sequence occurred in Central Italy on 2016–2017 pointed out that small-sized landslides such as falls and slides affecting rocky slopes, as well as earth slides and ground cracking, can have a significant impact on infrastructures that cannot be neglected in a multi-risk perspective, (Martino et al. 2019), needing to a high-resolution field surveying (EMERGEO Working Group 2010; Martino et al. 2017; Pucci et al. 2017). Over wider times, the coverage and completeness of historical data cannot match the adequacy of the event-based ground effects inventory defined in recent times. Nevertheless, historical data enrich the catalogues over a long time interval, which is fundamental for quantitative hazard assessment (Jibson 1996).

Long-lasting catalogues of effects are fundamental to reconstructing the seismic history of a site, as well as the magnitude of seismic events and the extent of the affected area. This can be achieved by using methods such as the lower-bound method (Keefer 1984) or frequency–area distribution (Tanyas et al. 2018; Papadopoulos and Plessa 2000). Historical chronicles play a significant role in earthquake-induced landslide inventorying and database reconstruction. For this reason, the most appropriate magnitude-distance relationships are represented by comprehensive catalogues that include the broadest record of historical and documentary information on earthquakes (Papadopoulos and Plessa 2000; Chen et al. 2012; Mikos et al. 2013; Martino et al. 2014).

Here is reported the most recent update of the Italian Catalogue of Earthquake-Induced Ground Failures - CEDIT, which inventories the effects induced by 215 earthquakes from 1117 A.D. up to 2025. Part of the CEDIT catalogue has been incorporated into the Global Earthquake-Induced Landslide (EQIL) one (Tanyas et al. 2017). This update includes new data, compared to the previous version released in 2014 (Martino et al. 2014), after surveying the effects of the 2016–2017 Central Italy seismic sequence, the 2018 Molise earthquake, the Mw 5.5 earthquake that occurred in November 2022 off the Adriatic coasts of the Marche region, and the 2025 Mw 4.6 Campi Flegrei earthquake, which, to date, represents the strongest volcano-induced earthquake recorded in the Phlegraean Fields area. Additionally, the systematic review of the 1908 Reggio and Messina earthquake and the 2009 L'Aquila earthquake, following Comerci et al. (2015) and EMERGEO (2010), has also been incorporated, as well as some missing data now reported by the new version of the CFTI Landslides (Italian database of the historical earthquake-induced landslides) following Zei et al. (2024a, b).

At the same time, focusing only on the earthquake-induced landslides, the spatial coverage and completeness of landslides induced by historical earthquakes are compared in this paper with those of the most recent landslides, triggered by the strongest seismic events and surveyed with accurate geolocation, whose quality is confirmed by the power-law correlation in their frequency-volume distribution (Martino et al. 2019). Based on the complete catalogues, which consist of either point or polygon features, it is possible to highlight regional distributions or peculiar far-field occurrences that can be explained by the predisposing roles of geostructural or topographic factors (Sepulveda et al. 2005; Meunier et al. 2008) or local seismic response (Delgado et al. 2011; Alfaro et al. 2012). In this sense, the recent seismic sequence that struck Central Italy in 2016 pointed out the relevance of surveying a distribution of earthquake-induced ground effects with a high resolution, which is suitable for infrastructural asset management and mitigation of geological risk to employ forward scenarios in a multi-hazard perspective (Martino 2017; Villani et al. 2018).

This 2025 CEDIT update moves beyond a simple catalogue of records, providing a framework that shifts the focus from merely documenting what was reported to leveraging what can be inferred for engineering geology. This approach yields two key outcomes. First, the inherent heterogeneity of historical and recent reporting was addressed by introducing an operational appraisal of completeness that accounts for survey visibility and its spatial coverage. Second, an Italy-specific reassessment of magnitude–maximum distance relationships was delivered for disrupted landslides,

providing an empirical envelope ready for regional screening and scenario delineation. Ultimately, the 2025 version is a clear evolution from previous releases, integrating the CEDIT directly into susceptibility modelling and multi-hazard risk workflows.

The CEDIT geodatabase

Since the 90 s the CEDIT catalogue, originally released by Delfino and Romeo (1997), was constructed in a project funded by the CERI (Research Centre for Prediction, Prevention, and Mitigation of Geological Risks of the University of Rome "Sapienza") through a detailed review of documentary sources and a systematic and structured logging of the inventoried effects, including their location. This project resulted in the first online version of CEDIT, edited by Fortunato et al. (2012) and hosted on a dedicated WebGIS, launched in 2012. Martino et al. (2014) thoroughly analysed the consistency of that database and defined the first Italian upper-bound curve for disrupted landslides (according to Keefer 1984). This curve was integrated with the available magnitude-distance empirical relations for liquefaction by Galli (2000), derived from Italian earthquakes that occurred between 1117 and 1990, along with evidence collected after the two 2012 Emilia-Romagna earthquakes.

The CEDIT catalogue has been integrated so far with: the effects of the seismic sequence of Central Italy occurred in 2016–2017; a few ground cracks and minor rock falls recorded after the 2017 Casamicciola (Ischia Island, NA) earthquake; the 2018 Mw 5.1 Molise earthquake (Martino et al. 2020a, b); the 2019 Mw 4.4 Balsorano earthquake. Finally, as a consequence of this work, the ground effects triggered by the 2022 Mw 5.5 Adriatic coast earthquake and two disrupted landslides induced by the 2025 Mw 4.6 Campi Flegrei earthquake are included.

Furthermore, an update regarding the 1908 Mw 7.1 Reggio and Messina earthquake, based on the review presented by Comerci et al. (2015), and the 2009 Mw 6.3 L'Aquila earthquake, also based on the EMERGEO (2010) report, was performed. Additionally, due to the publication of the updated version of the CFTI Landslides catalogue by Zei et al. (2024a, b), which provides information on earthquake-induced landslides up to the 1997 Umbria-Marche seismic event, a comparison between the two databases was carried out. This comparison allowed to report, in the updated version of CEDIT, 108 earthquake-induced landslides associated with 37 previously uncatalogued seismic events, as well as 105 earthquake-induced landslides linked to seismic events already reported in the catalogue.

The here presented 2025 CEDIT release contains all the latest updates and is fully accessible and open through a server platform that provides downloadable data or accessible for visualisation via dedicated Web Map Services (WMS). The most updated release of CEDIT is also optimised for portable devices and can be freely accessed and used in the field through an integrated geolocation tool. It was structured using a WebGIS application developed with Lizmap, an open-source software that enables QGIS® Desktop to create web map applications linked to a PostgreSQL database. The WebGIS homepage is accessible through the geodatabase page of the CERI Research Centre at https://gdb.ceri.uniroma1.it/. The WebGIS displays the entire catalogue content, including both earthquakes and their induced ground effects, on the OpenStreetMap® basemap of Italy. Earthquake-induced ground effects are represented by coloured point indicators based on the type of effect, while earthquake epicentres are shown with a graduated size indicator corresponding to the event's magnitude. The new version of the catalogue explicitly reports geolocation uncertainty by using a circle centred on the point, with a radius inversely proportional to the localisation accuracy.

The current CEDIT manages an Entity-Relationship (E-R) geodatabase, in which each earthquake, from 1117 A.D. to 2025, is associated with its induced ground-failure effects. In the first version of the catalogue, seismic effects induced by earthquakes were inventoried by examining historical documents and published literature (Prestininzi and Romeo 2000). On the other hand, ground effects induced by recent seismic events were directly surveyed in the field by the CERI technical team, as well as by collecting information from professionals and social and technical communities, who were allowed to submit reports of specific effects using an online interface.

In general, the E-R geodatabase is structured into five main tables, named "Earthquakes", "Effects", "Phrases", "Bibliography", and "Surveys". The first table, "Earthquakes", collects all the seismological information on the events, chronologically ordered, with which the earthquake-induced ground effects are associated. These effects are recorded in the "Effects" table, either inventoried from historical sources or directly detected on the ground. Each effect entry includes geographic, geological, and seismological information, such as geographical coordinates, effect type, epicentral distance, macroseismic intensity (MCS scale) attributed to the site, main lithology involved, and a georeferencing class. Regarding the historical effects, the "Phrases" table contains excerpts of sentences taken from historical sources, which describe, with varying degrees of accuracy, the ground effects produced by the earthquakes. Additionally, in the "Bibliography" table, each sentence is linked to its corresponding bibliographic source. For effects directly surveyed in the field, information such as the survey date, the names of the surveyors, and a photograph of the effect are listed in the "Surveys" table. The

five main tables are linked thanks to a geodatabase's primary key, identified in the ID of the earthquake. A detailed description of the relational structure of the database is reported in Caprari et al. (2018).

Since 2016, due to the specifically planned direct surveying of ground effects, each seismic effect was associated with additional information such as the volumetric class, the type of slope from which it was triggered (i.e., natural slope or man-made cuts), and an assessment of the actual or potential interference with the road network or anthropogenic structures.

Regarding the typologies of earthquake-induced effects, these are collected in the database according to five main categories: (i) landslides; (ii) ground cracks; (iii) liquefactions; (iv) surface faulting; and (v) ground changes (Fortunato et al. 2012). These main categories are further divided into subcategories; in particular, the landslides are classified according to the type of effect, kinematics, and material involved (based on Varnes 1978a, b).

To ensure a reliable geolocation of the inventoried effects, five different classes of georeferencing were distinguished in accordance with Italy's hierarchical division of administrative units (Martino et al. 2014). An estimated error was assigned to each class, from the most to the least accurate: (i) Class 5: site coordinates (high-quality location from historical documents or GPS measurements) associated with no error or a negligible one; (ii) Class 4: administrative locality coordinates (area extent of square kilometres) associated with an average error of 1 km; (iii) Class 3: main town/village coordinates (area extent of tens of square kilometres) associated with an average error of 3 km; (iv) Class 2: municipality coordinates (area extent of hundreds of square kilometres) associated with an average error of 10 km; (v) Class 1: province coordinates (area extent of thousands of square kilometres) associated with an average error of 30 km. Consequently, ground effects related to the most recent earthquakes and geolocated with GPS belong to Class 5 of geolocation, while ground effects linked to older earthquakes, located on the basis of historical sources, belong to lower resolution location classes. For this reason, CEDIT also includes multiple earthquake-induced ground effects, i.e., multiple effects that occurred in the aftermath of the same earthquake and are linked to the same geographical coordinates (e.g., if falling into geolocation class 1, 2, or 3).

From an engineering geology point of view, the CEDIT catalogue is not only a static dataset but also provides a structured database of earthquake-induced ground effects that can support: (i) the validation and calibration of susceptibility and multi-hazard models, (ii) the scenario-based assessments of expected affected areas, (iii) a rapid post-event situational awareness of the environmental damages. The database attributes (effect type, spatial coordinates with associated location-quality classes, and source information) allow users to filter records by uncertainty level and intended application, facilitating integration into standard GIS workflows.

Last inventoried events: the 2022 Mw 5.5 Adriatic coast and the 2025 Mw 4.6 Campi Flegrei earthquakes

Among the last earthquakes with inventoried ground effects, the CEDIT includes the one that occurred on November 9th, 2022, at 06:07:24 UTC The Mw 5.5. event struck the coastal area of the Marche region between the cities of Pesaro and Ancona (Famiani et al. 2025). The earthquake originated from a compressive fault, with an offshore epicentre approximately 30 km off the coast, suggesting the possible activation of onshore earthquake-induced ground effects. The earthquake was felt in a wide portion of the Marche coastal region, including the sea-active cliffs of the Mt. Conero promontory and the San Bartolo coastal slopes, which are situated within the foreland zone of the Apennine chain. These areas are geologically composed of both limestones and clayey lithologies, which outcrop over steepened slopes (Troiani et al. 2020; Piacentini et al. 2021; Marmoni et al. 2023; Fullin et al. 2024).

A field survey was carried out inland over two days following the seismic event within a 60-km-wide buffer centred on the epicentral area. This short-time response allows for the minimisation of the potential influence of subsequent rainfall, deferred failure controlled by swell events, or aftershocks that could have caused interference among the events, as experienced during the 2016–2017 Central Italy seismic sequence. The field surveying allowed the inventorying of 18 earthquake-induced ground effects, represented by landslides and divided into different mechanisms, as follows: 7 rock falls, 6 topples, 2 rock wedge slides, 1 earth slide, 1 debris fall, and 1 debris slide (Varnes 1978a, b; Fig. 1).

A preliminary analysis of the effect distribution indicates that the totality of the landslides was triggered beyond the expected Maximum Epicentral Distance (MED). For a Mw 5.5 earthquake, the MED for disrupted landslides is typically around 40 km, according to Keefer (1984), and about 28 km, according to Martino et al. (2014), which considers MED values more representative of Italian environmental conditions. Instead, the MED for coherent landslides does not exceed 12 km, again according to Keefer (1984). The landslides observed during the survey were all located beyond their respective MEDs and up to 60 km from the epicentre, suggesting that specific geological or geomorphological predisposing and preparatory factors, including seismological parameters, explain

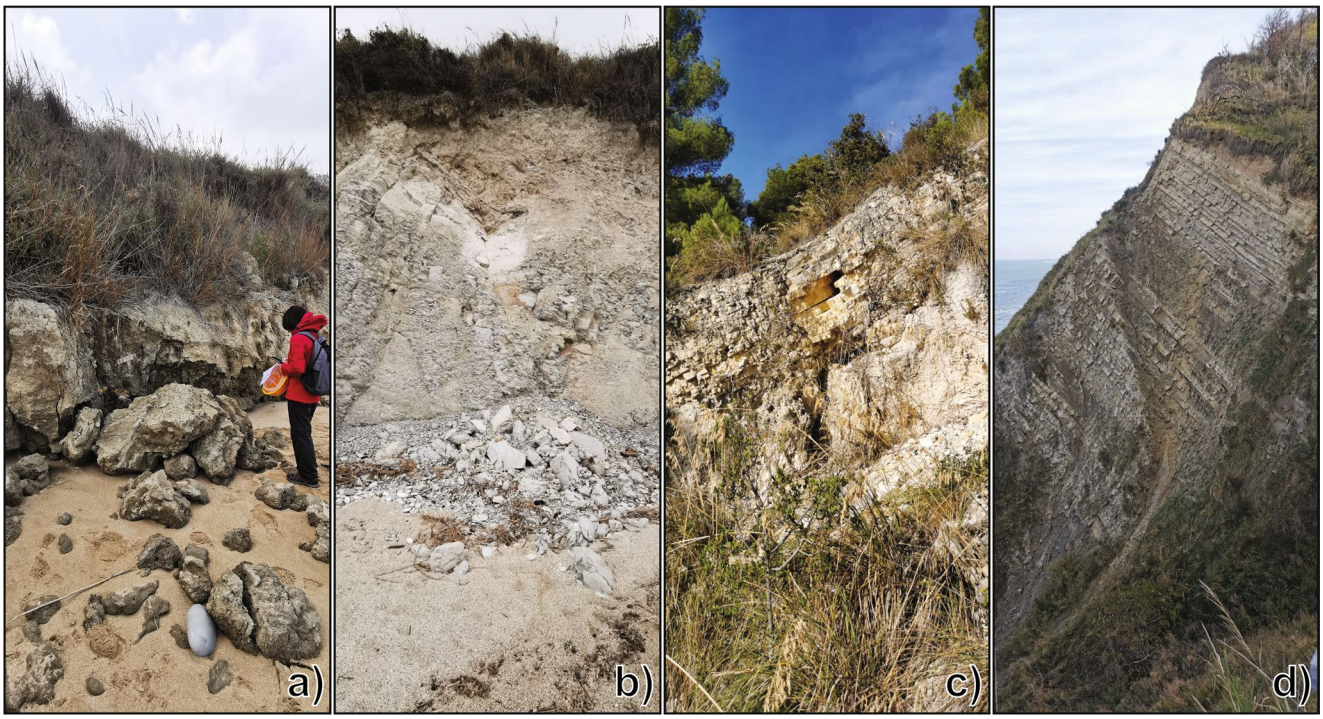

Fig. 1 Examples of earthquake-induced landslides from the field survey. Topples (**a**) and rock wedge slides (**b** and **c**) were inventoried at Mezzavalle beach (**a** and **b**) and at Passo del Lupo slope (**c**) (Conero promontory); example of rock fall catalogued at Fiorenzuola di Focara slope at San Bartolo promontory (**d**) (photo credits: CERI working group)

their occurrence beyond the expected distance. In the case of the earthquake-induced landslides caused by the 2022 Adriatic coast seismic event, the former can be represented by the sub-vertical attitude of the marine cliffs composed of flysch and clayey lithologies, while the latter ones are found in progressive weathering due to the salty aerosol related to the proximity to the sea.

The most recent earthquake inventoried in the CEDIT occurred on June 30th, 2025, at 10:47:11 UTC, with a Mw 4.6, which struck the coastal area of the Pozzuoli gulf, located in the Campi Flegrei volcanic field area (Naples). The earthquake is part of an ongoing seismic swarm associated with an active bradyseism uplift, a phenomenon characterised by vertical ground movements caused by the dynamics of magmatic and hydrothermal fluids within the shallow crust (Del Gaudio et al. 2010; Chiodini et al. 2016). The Campi Flegrei area is a large resurgent caldera formed by several explosive eruptions during the Late Quaternary, including the Campanian Ignimbrite (~39 ka) and the Neapolitan Yellow Tuff (~15 ka), and is considered one of the most hazardous volcanic regions in Europe due to its high population density (Orsi et al. 1996). Tectonically, the caldera is located within a complex extensional setting resulting from the interaction between the Apennine compressional system and the opening of the Tyrrhenian back-arc basin (Vitale and Isaia 2014). The seismicity is typically shallow (≤5 km depth) and reflects the interplay between fault reactivation, fluid overpressure, and stress perturbations induced by magma and gas accumulation (D'Auria et al. 2011; Petrosino et al. 2018, 2020). The June 2025 event, among the strongest recorded in the area since the 1980s, induced two rock falls from the coastal cliffs located in Isola Pennata and in Isolotto del Castello di Baia, just 1.9 and 1.25 km from the epicentre respectively. These two effects were not directly surveyed in the field, but the detailed information provided by media and web sources allowed their inclusion in the CEDIT with class 5, the highest in terms of georeferencing accuracy.

Content and statistics of the 2025 release

The current CEDIT includes 4256 earthquake-induced ground effects that occurred in 1012 administrative localities, related to 215 earthquakes (Fig. 2). More specifically, 2457 ground effects fall under the landslides macro-category, representing 58% of the total collected effects. Ground cracks account for 981 ground effects, making up 23% of the total. A total of 486 ground effects are due to liquefactions, constituting 11% of the inventory, while ground changes account for 194 effects, representing 5%. Finally, 138 ground effects belong to the surface faulting macro-category, making up 3% of the entire catalogue. The administrative localities where ground failures occurred are

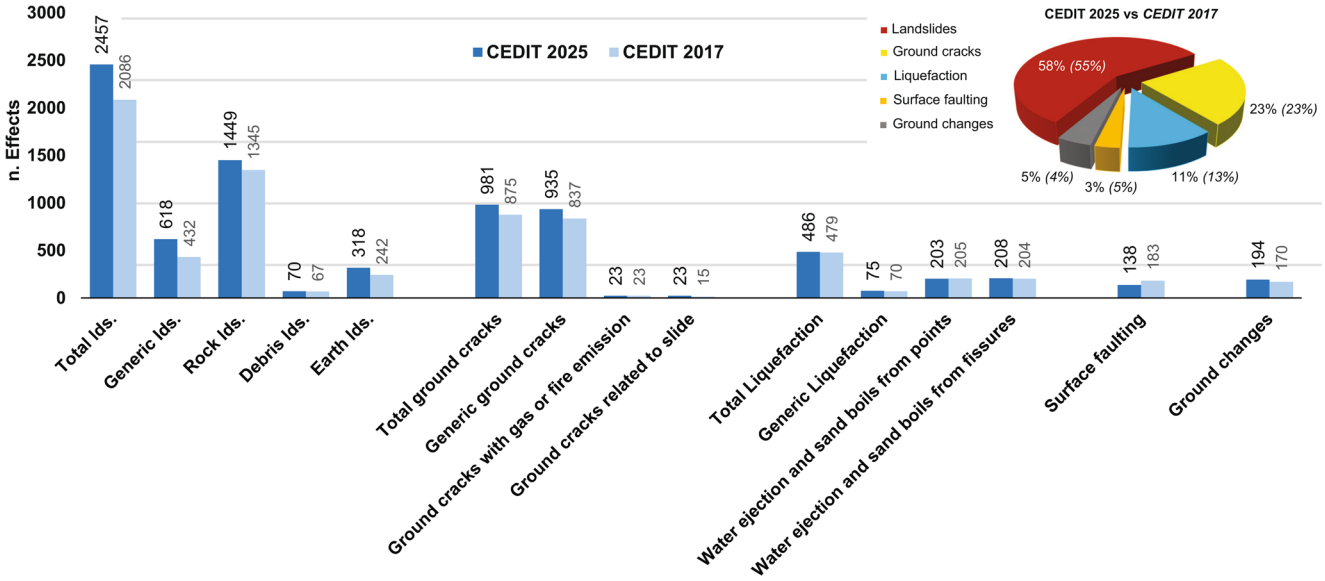

Fig. 2 Bar chart showing the number of earthquake-induced ground effects inventoried in the 2025 release of the CEDIT, compared with the previous 2017 release by Caprari et al. (2018). The pie chart shows the relative percentages for the five macro-categories of inventoried ground effects (in brackets, the percentages are from the 2017 release by Caprari et al. 2018)

identified by an administrative code attributed by the Italian National Institute of Statistics (ISTAT).

Based on the data inventory, the CEDIT is nowadays the most up-to-date and comprehensive database of earthquake-induced ground effects currently available in Italy. This is because, compared with other available catalogues for the Italian territory, CEDIT appears to have the highest resolution and the most significant temporal coverage (also in terms of recent updates) and contains information on all categories of effects induced by earthquakes. Figure 3 illustrates the spatial distribution of the earthquake-induced ground effects inventoried in the 2025 release of the CEDIT and the earthquake epicentres, according to the seismogenic sources from the DISS catalogue (DISS Working Group 2021).

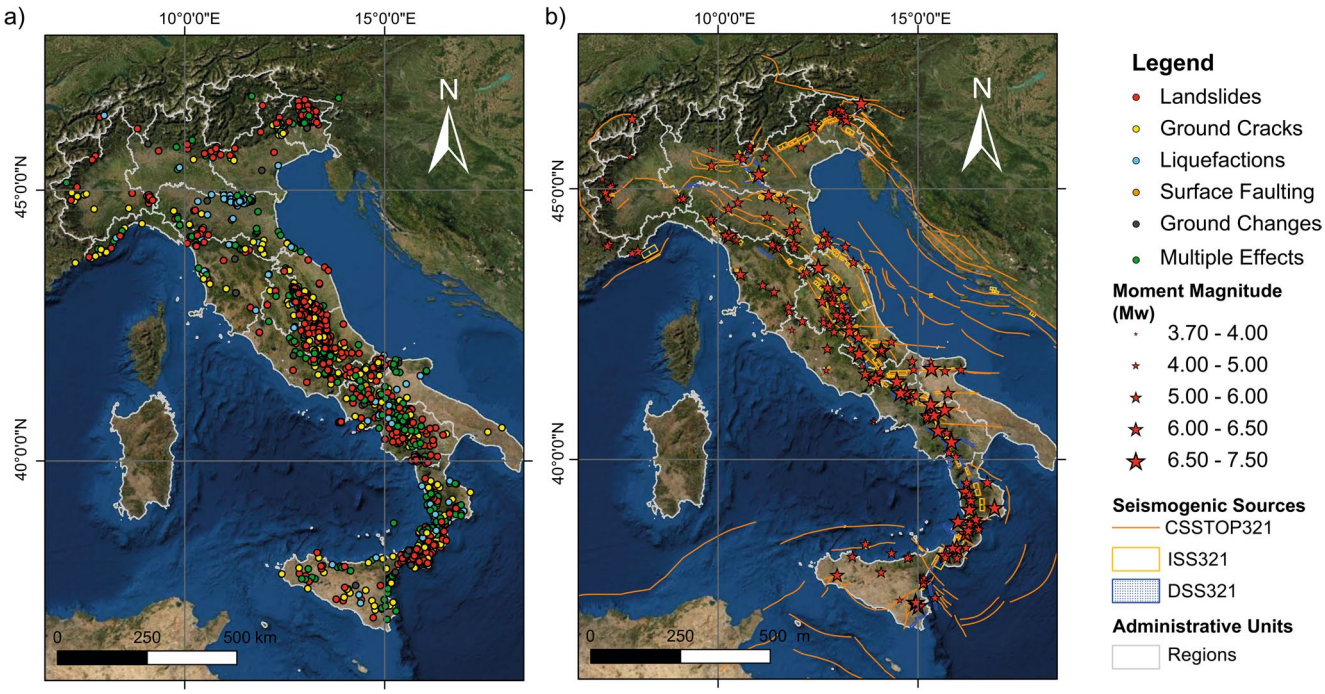

Fig. 3 Location of the earthquake-induced ground effects (**a**) and epicentres of the triggering earthquakes (**b**) inventoried in the CEDIT catalogue. The spatial distribution of the main seismogenic sources from the DISS and ITHACA databases is also reported (**b**)

The earthquakes associated with the inventoried ground effects reflect the characteristic seismicity of the Italian territory, with moment magnitudes (Mw) ranging from 2.9 to 7.32 (source: CPTI https://emidius.mi.ingv.it/CPTI/ - Fig. 4a). Specifically, magnitudes from 5.5 to 6.0 roughly correspond to an epicentral intensity of VIII on the Mercalli-Cancani-Sieberg scale (MCS). The decrease in the number of earthquakes for magnitude classes below 5.5 and above 6.5 represents a systematic bias, attributed to the lower propensity to trigger earthquake-induced ground effects and the lower frequency of occurrence, respectively. While hypocentral depth can significantly influence ground response (and induced effects), almost all the inventoried earthquakes are reasonably shallow (depth less than 30 km), consistent with the seismotectonic framework of Italy (Meletti et al. 2000).

As it regards the relationship between earthquake-induced ground effects and site macroseismic intensity defined by the MCS standard macroseismic scale, the abundance of effects vs. number of earthquakes in the respective MCS epicentral intensity class shows an exponential increase in the frequency of effects with increasing epicentral intensity (Fig. 4b). The absolute and relative frequency of ground failures in the CEDIT highlights a peak in epicentral intensity corresponding to values 9–10, which can be attributed to the Central Italy 2016–2017 seismic sequence. During this sequence, detailed field surveys led to the direct detection of 770 landslides of various sizes, representing a significant exception within the catalogue's dataset. Figure 4c shows the relative distribution of earthquake-induced ground effects concerning local MCS intensity. A modal value is observed around MCS intensity 8, except for surface faulting, which is more prevalent in MCS intensity 9. The latest catalogue update confirms a triggering threshold for earthquake-induced ground effects ranging from MCS intensity 5 to 6 for landslides and about one degree higher (MCS intensity range equal to 6–7) for all other types of ground failure.

Consistency and completeness of the CEDIT catalogue

The CEDIT refers to historical sources or literature data, which indicate the location of different types of ground effects at different degrees of accuracy. The spatial distribution of earthquake-induced ground effects, classified by type and quantity per municipality (Fig. 5), is closely linked to the inventoried seismogenic sources (see DISS and ITHACA databases and Fig. 2). Spatial gaps are intrinsically correlated with inventory deficiencies, the absence of relevant seismic events, and varying susceptibility of the territory to experiencing instabilities.

The accuracy of ground effect locations has varied over time, improving in recent years with the availability of satellite images and direct field observations. During the 2016–2017 Central Italy seismic sequence, for the first time, detailed field surveys were carried out, inventorying earthquake-induced ground effects with a very high level of accuracy (Q5) in contrast to what can be retrieved from historical documentary sources (Fig. 6a).

The CEDIT database significantly increased over time, exceeding 4000 recorded effects so far, with more than 80% of these effects occurring from the 19th century onward. The temporal distribution of these effects also highlights the CEDIT dataset's intrinsic inhomogeneity, reflecting an increasing number of inventoried effects corresponding with strong earthquakes (Fig. 6).

The CEDIT provides a comprehensive overview of the state of knowledge on the effects that have occurred or are expected along the Italian peninsula. In this context, given the extensive dataset and diverse sources of information, a preliminary review of the catalogue was conducted to assess its completeness, particularly for effects coming from historical earthquakes (where only documentary sources are available) and recent seismic events, where direct field surveys or remote sensing data were used. To this aim, the consistency of the database was evaluated by analysing the absolute frequency of ground effects and spatial coverage, with a separate analysis of the historical effects and those surveyed in the 20th and 21 st centuries, each with varying degrees of accuracy.

The analysis of the cumulative number of effects relative to epicentral distance reveals a higher abundance in epicentral areas for earthquakes that occurred since 1997 (e.g., the Umbria-Marche Earthquake), a time-interval during which direct surveys were carried out, and even smaller-scale effects were more systematically documented (Fig. 7). Exceptions include the 1908 Reggio and Messina earthquake (Mw 7.1), which underwent a historical documentary revision process based on Comerci et al. (2015), leading to a significant increase in the catalogued earthquake-induced ground effects in the current version of CEDIT, and the 1980 Irpinia earthquake (Mw 6.9), which occurred during a period when more accurate surveys began to be performed, with the induced ground effects being directly mapped onto topographic maps. Figure 7 shows that the inventory of earthquake-induced ground effects from historical earthquakes contains no more than 25 effects per event, with only a few outliers.

The distance to the furthest effect and the affected areas were also analysed to better understand the spatial distribution of ground effects. The analysis of the number of effects and their spatial distribution relative to earthquake magnitude for each seismic event was conducted by normalising

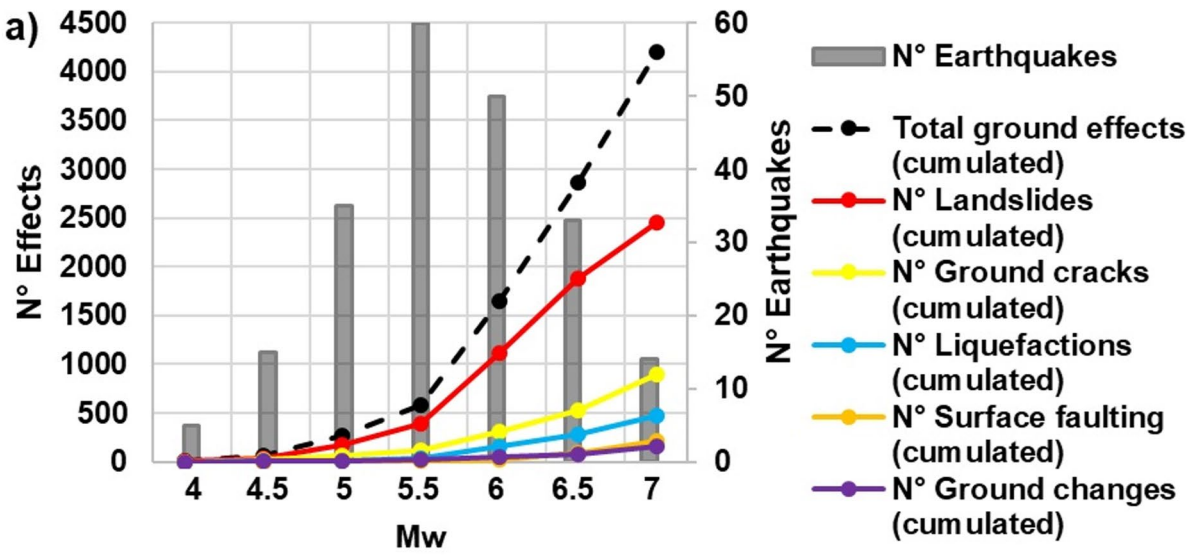
a)
N° Effects
N° Earthquakes
Mw
N° Earthquakes
Total ground effects (cumulated)
N° Landslides (cumulated)
N° Ground cracks (cumulated)
N° Liquefactions (cumulated)
N° Surface faulting (cumulated)
N° Ground changes (cumulated)

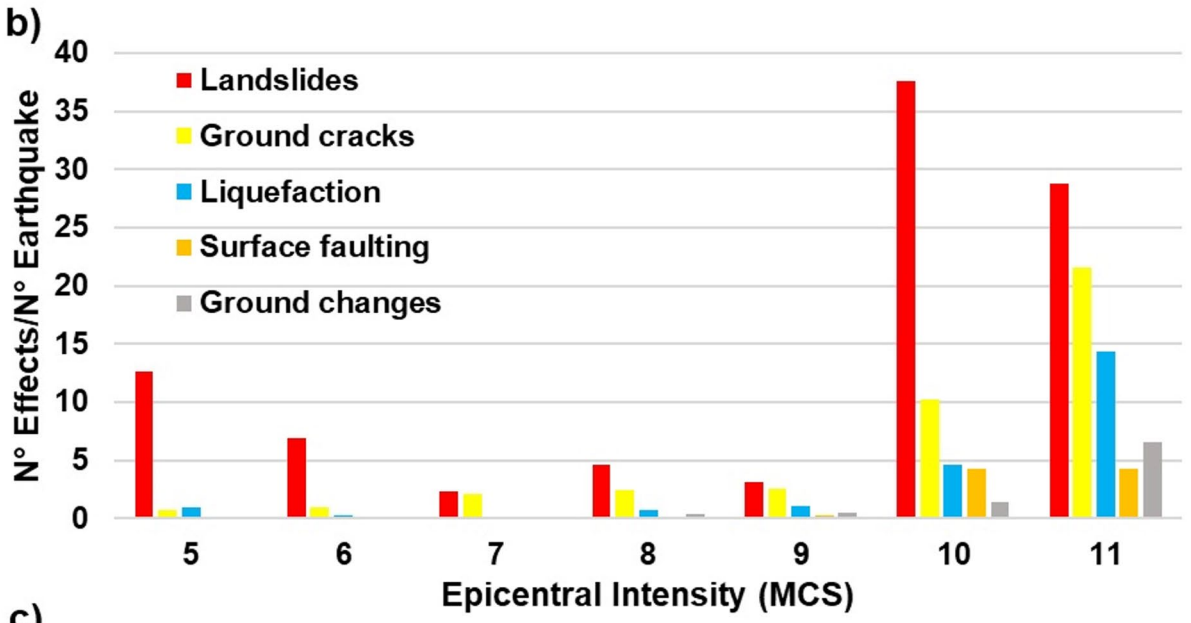
b)
N° Effects/N° Earthquake
Landslides
Ground cracks
Liquefaction
Surface faulting
Ground changes
Epicentral Intensity (MCS)

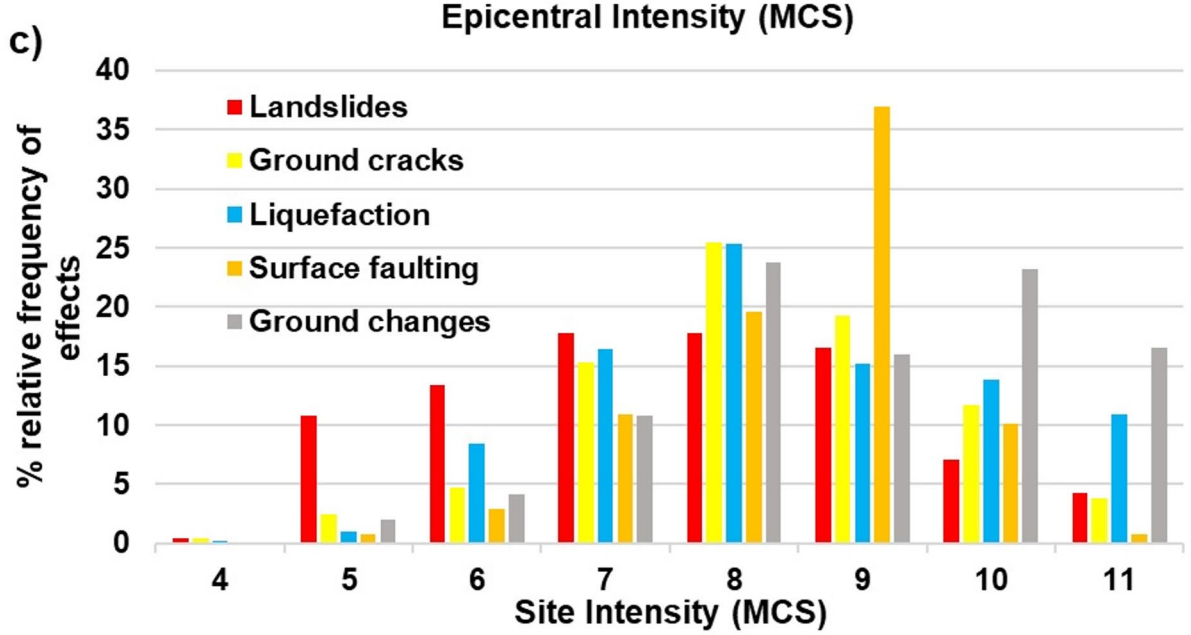
c)
% relative frequency of effects
Landslides
Ground cracks
Liquefaction
Surface faulting
Ground changes
Site Intensity (MCS)

Fig. 4 Number of earthquakes vs. moment magnitude (Mw) reported in the CEDIT. The class interval is fixed at 0.5 Mw (upper limit included and the lower limit excluded, xi-1 < x ≤ xi). The number of triggered earthquake-induced ground effects for each magnitude class is also reported (**a**). Absolute frequency of ground failures by seismic event vs. epicentral intensity (MCS scale) reported in the 2022 release of CEDIT (**b**); relative frequency of ground failures vs. local intensity (MCS scale) reported in the 2022 release of CEDIT (**c**)

the number of ISTAT localities affected by ground effects with the total of localities falling within the Keefer maximum expected distance (Keefer 1984), which is considered a proxy for spatial completeness. The normalised ratio of administrative localities affected by ground instabilities to the total number of localities within the Mw-specific Keefer distance shows that, apart from total number of effects, the historical earthquakes impacted a similar number of localities compared to those occurring since the XX century (Fig. 8a). Here, "administrative localities" are used as a stable territorial reference layer and should not be interpreted as "populated places" only: the ISTAT partition covers the entire national territory and also includes case sparse (dispersed localities), which account for a large fraction of Italy's surface. This knowledge level is largely attributed to the meticulous census efforts of municipal and clerical archivists, who thoroughly documented evidence of failures in both large cities and small villages. While the reference layer covers the entire territory, the resulting metric primarily serves as a proxy for reporting effort. Physical completeness is often hindered by accessibility issues or uneven documentation density, particularly in complex terrain. To account for this, we treat the ratio as a comparative baseline, complemented by event-specific visibility checks. Using administrative units as a spatial framework maintains consistency with the methodology used by Martino et al. (2014) in prior CEDIT analyses.

The distribution of inventoried ground effects reveals an increasing data gap with rising earthquake magnitude, indicating an intrinsic limitation in the inventory's completeness, likely due to the low frequency of occurrence of very strong earthquakes in the Italian territory. Beyond this, starting from the XX century, there has been a noticeable increase in the number of seismically induced ground effects recorded for each earthquake, following a trend that can be approximated by an incremental linear function as the magnitude increases (Fig. 8b).

Focusing on the "landslide" effect alone and from a statistical point of view, achieving full spatial coverage for landslide datasets is challenging due to technical limitations in surveying methods. Due to the limitations in the available attributes associated with landslide effects, such as quantitative volume or areal estimates for historical events, the analysis of frequency versus area distributions (Malamud et al. 2004; Tanyas et al. 2018) was not undertaken. This is also inherently due to the criteria for mapping adopted in the CEDIT, where ground effects are recorded as point elements to provide a standard dressing to the information from historical documentary sources and direct survey datasets. The test of inventory completeness for the 2016 Amatrice earthquake, performed by analysing the frequency versus volume distribution, highlights the inventory's completeness, demonstrating a negative power-law correlation with a coefficient (β) of 0.99 (Martino et al. 2019). This parameter aligns with and is comparable to those proposed by Marques (2008), Malamud et al. (2004), and Brunetti et al. (2009), and is considered acceptable, largely due to the inclusion of a significant fraction of smaller-sized effects that extend the range of effect volumes (Malamud et al. 2004).

Insights on catalogue completeness from the 2016–2017 Central Italy seismic sequence

The spatial distribution of earthquake-induced ground effects following the three main shocks of the 2016–2017 Central Apennines seismic sequence was analysed to discuss potential completeness issues in catalogues like CEDIT, which integrate both historical and recent data. In this case, the completeness guaranteed by the field surveying was evaluated using GIS spatial analysis tools, demonstrating that interference among successive mainshocks can occur, potentially affecting the completeness of the effects induced by one of the earthquakes in the sequence or leading to incorrect cataloguing. This issue is crucial for the quantitative analysis of interference between subsequent earthquakes in a sequence (Ferrario 2019; Burrows et al. 2023). A delayed survey or reliance solely on remote inventorying would overlook ground cracks related to faulting or landslides and the frequent rock falls on hard lithologies from natural cliffs and anthropogenic cuts, especially when they are small. These features are often quickly obliterated by human restoration efforts or by weathering and water runoff in the days following the event.

The 2016–2017 Central Apennine seismic sequence struck a wide area encompassing the Lazio, Marche, Umbria, and Abruzzo regions. The sequence began with the Mw 6.0 Amatrice earthquake on August 24, 2016 (hereafter AMA), followed by the Mw 5.9 Castelsantangelo sul Nera earthquake on October 26, 2016 (hereafter CSN). This was accompanied by thousands of seismic events, including the strongest, which reached Mw 6.5 on October 30, 2016, in Norcia (hereafter NOR). The main shocks concluded in January 2017 with the Mw 5.5 Capitignano earthquake (hereafter CPT). The three mainshocks of 2016 were responsible for most of the casualties, the building damages (Galli et

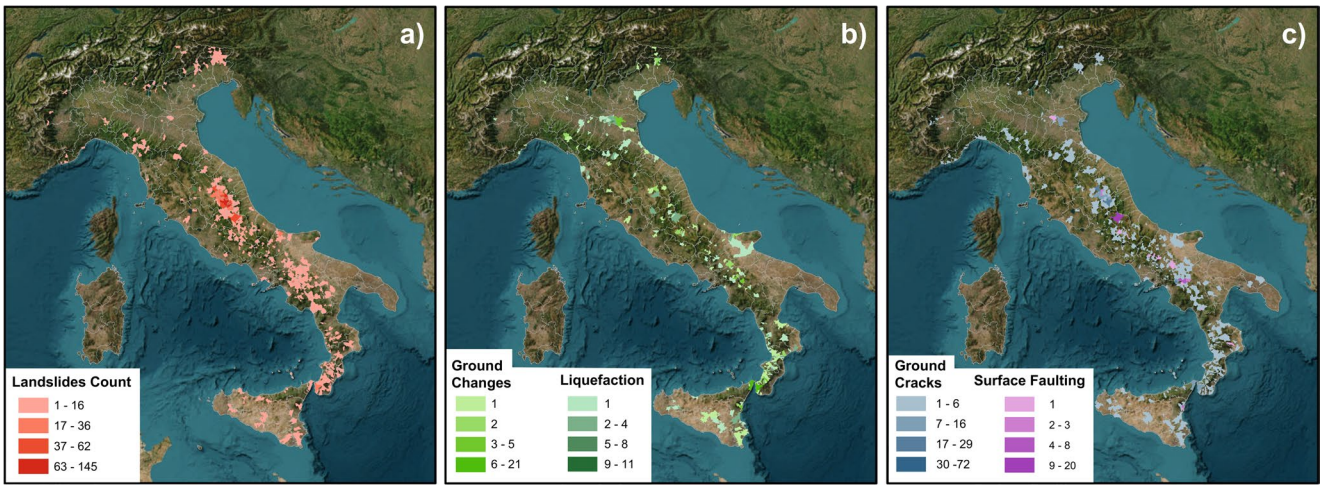

Fig. 5 Ground effects distribution within municipalities over the Italian territory. Count of Landslides (**a**), Ground changes and liquefaction (**b**), and ground cracks and surface faulting (**c**) are reported

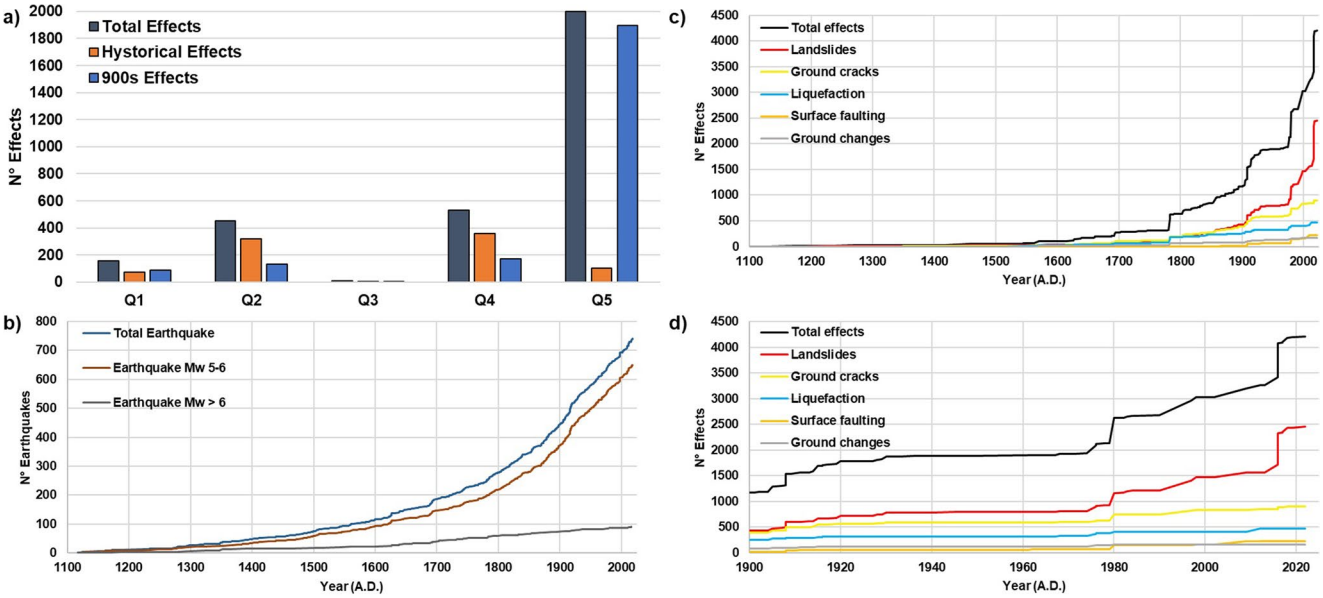

Fig. 6 Number of earthquake-induced ground effects categorised for geolocation quality (from Q1-Q5, according to Martino et al. 2014) (**a**); evolution of the earthquake in the Italian peninsula (**b**) and of the number of earthquake-induced ground effects from 1100 A.D. to date. The zoom starting from the 20th century for ground effects only (**d**) is also provided

al. 2017), the infrastructure destruction (Sisti et al. 2019), and the impact on cultural and monumental heritage (Hofer et al. 2018). They also triggered a significant number of ground effects, primarily landslides (Martino et al. 2019).

The CEDIT Working Group surveyed most of the induced effects through both in-field and remote sensing methods immediately after each main shock (Martino et al. 2017, 2022), identifying almost exclusively landslides as the type of effect produced by the earthquakes. Generally, remote sensing surveys allowed for the inventory of slope-scale ongoing deformations, even in impervious and inaccessible areas (Sato and Harp 2009). However, they have significant limitations, as they are not always effective in detecting landslides with small volumes, especially when small rock blocks are involved. Aerial photo monitoring and optical satellite detection of landslides is often hindered by atmospheric conditions, which can delay accurate geolocation of ground effects for several days following an event (Wasowski et al. 2011). Such inventorying can be achieved with radar sensors (Burrows et al. 2023), even with a coarser resolution. This highlights that in-field mapping remains an essential, integrative technique for detecting earthquake-induced effects such as ground cracks and minor, yet frequent, landslides, as demonstrated by numerous research groups (EMERGEO Working Group 2016; 2018; Martino et al. 2017, 2019, 2020a, b). Also, in-field surveying can be affected by several

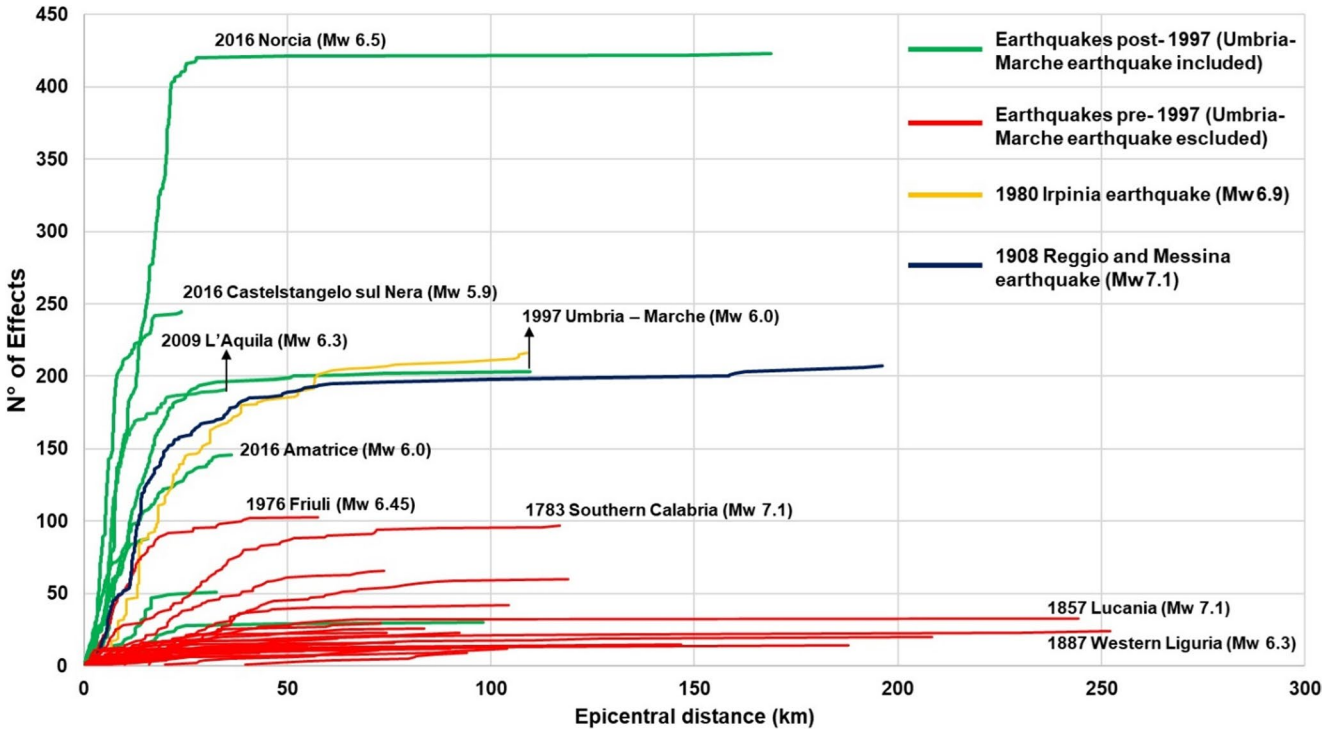

Fig. 7 Cumulative number of effects vs. their epicentre for each earthquake inventoried into the CEDIT. Directly surveyed recent events (starting from the 1997 Umbria-Marche Mw 6.0 earthquake; green lines) and historical earthquakes reported by document-based analysis of historical sources (before the 1997 Umbria-Marche Mw 6.0 earthquake; red line) are distinguished. The two exceptions concerning the earthquake of 1908, Reggio and Messina, Mw 7.1 earthquake, and the 1980 Irpinia, Mw 6.9 earthquake, are highlighted in different colours (blue and yellow, respectively)

limits and potential biases, with the most critical being the inability to comprehensively survey all epicentral regions of interest. This challenge is primarily due to accessibility constraints during the emergency phase, which is influenced by the sparse distribution of road and path networks, road closures, and the inherent limitations in visibility imposed by the complex orography of the felt region.

Regarding the 2016–2017 seismic sequence, the number of seismic effects inventoried in the CEDIT is notably high, particularly relative to the surveyed area. However, it is important to note that not all regions were comprehensively covered by field surveys due to the aforementioned reasons. This is demonstrated through the application of a visibility test through a GIS-based analysis, which distinguishes between visible and obscured areas from specific observation points. The results of the visibility test indicate a significant distribution of detectable zones in proximity to the epicentral areas, suggesting thorough field mapping of those regions (Fig. 9). In contrast, the non-visible areas are predominantly associated with inaccessible regions due to factors such as (i) inaccessible location, (ii) lack of roads, and (iii) logistical constraints during the emergency phase, including landslides that obstructed road access.

The 2016–2017 dataset was further analysed by examining the frequency distribution of earthquake-induced ground effects relative to the epicentral distance to better assess interference effects among earthquakes that occur close in time. As established in the literature, induced seismic effects typically decrease as the distance from the epicentre increases (Keefer 1984, 2002; Rodriguez et al., 1999, Martino et al. 2017). To verify this hypothesis and assess the completeness of the survey, the number of seismic effects was calculated as a function of increasing epicentral distance, grouped into 5 km intervals. For the AMA and CSN cases, the number of seismic effects exhibited a linearly decreasing trend with increasing distance from the epicentre (Fig. 9). At the same time the Landslide frequency Index (LI; i.e., the ratio of the number of effects in each distance class normalised by the total number of effects to the areal extent of each class normalised by the total survey area) also displayed a monotonic decreasing trend. In contrast, the NOR earthquake, which occurred just 4 days later than the CSN one, presented a different frequency distribution characterised by a lower abundance of seismic effects within the first 5 km from the epicentre and a non-exponential trend in the LI. Such an anomalous pattern is likely ascribable to the previous occurrence of both the CSN and AMA earthquakes, which may have altered the seismic landscape of the NOR event, effectively reducing the number of triggerable seismic effects in its

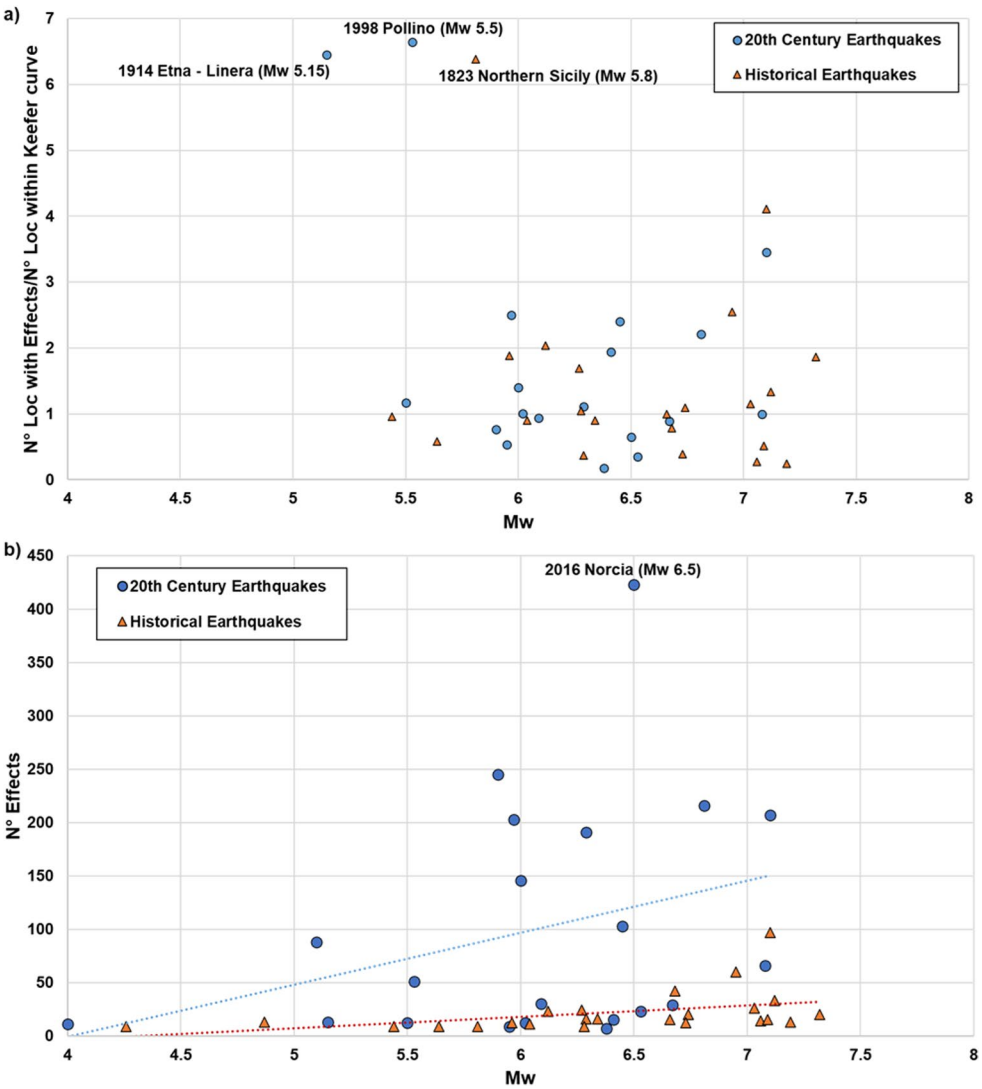

Fig. 8 Ratio between the number of localities with inventoried Effects and the number of localities falling within the maximum expected distance provided by the Keefer curve for a given magnitude (Keefer 1984). Effects reported by chronicles for historical earthquakes and recent events since the 20th century are shown (**a**). Number of effects vs. magnitude of the triggering earthquake. Effects reported by chronicles for historical earthquakes and surveyed events since the 20th century are shown. The dashed line represents the trend and emphasises the difference between historical earthquakes and more recently occurred ones (**b**)

epicentral region. The areal overlapping of the earthquake-induced effects becomes evident when circular areas with increasing radius, ranging from 5 to 10 km, centred on the earthquake epicentres that have a geodetic distance of 9 km between them (Fig. 10). Several landslides were documented following the CSN events, particularly within the innermost sector of the epicentral area of the subsequent NOR earthquake. A significant concentration of rock fall events was observed within a 10 km radius, especially along the SP134 road from Visso to Castelsantangelo sul Nera. This interference reduces the availability of unstable rock blocks prone to failure.

Multiple reactivations of landslides were also documented throughout the entire seismic sequence, with cumulative seismically induced displacements observed. Notable examples include the rototranslational landslide in Ussita (classified as a coherent landslide according to Keefer 1984), which experienced several reactivations and the detachment of several rock blocks from the vertical cliff on the northern slope of Mt. Bove (Fig. 11).

The 2016–2017 seismic sequence has underscored the challenges of cataloguing earthquake-induced effects, particularly highlighting the risk of census incompleteness, which becomes increasingly significant as the scale of effects diminishes, especially without detailed surveys. Although relatively small in volume, rock failures from roadcuts substantially caused direct damage and contributed to cascading effects that influenced both emergency response and recovery phases. In such a context, integrating remote sensing techniques with comprehensive surveys of surface effects, including ground cracks and surface faulting, which are often not discernible from satellite imagery, proves essential for creating complete and reliable inventories necessary for accurate forecasting and evaluation of future scenarios of earthquake-induced landslides failure, that would learn from both strong earthquakes and weaker events.

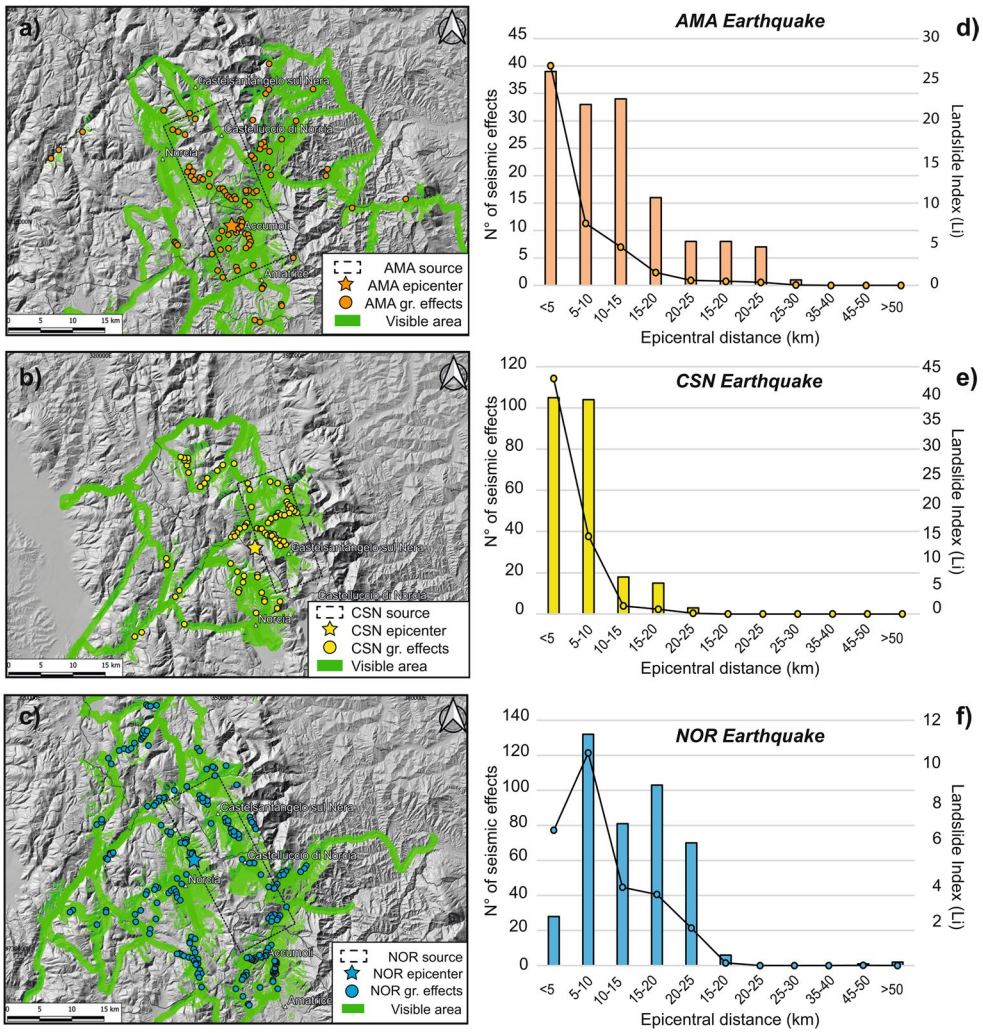

Fig. 9 Maps derived by the GIS-based Visibility tool test for the distribution of the effects related to the Amatrice (AMA) (**a**), Castelsantangelo sul Nera (CSN) (**b**) and Norcia (NOR) (**c**) earthquakes, with respect to the epicentral distance (**d**, **e**, **f**). Green shapes represent visible territory based on the route taken during the field surveys

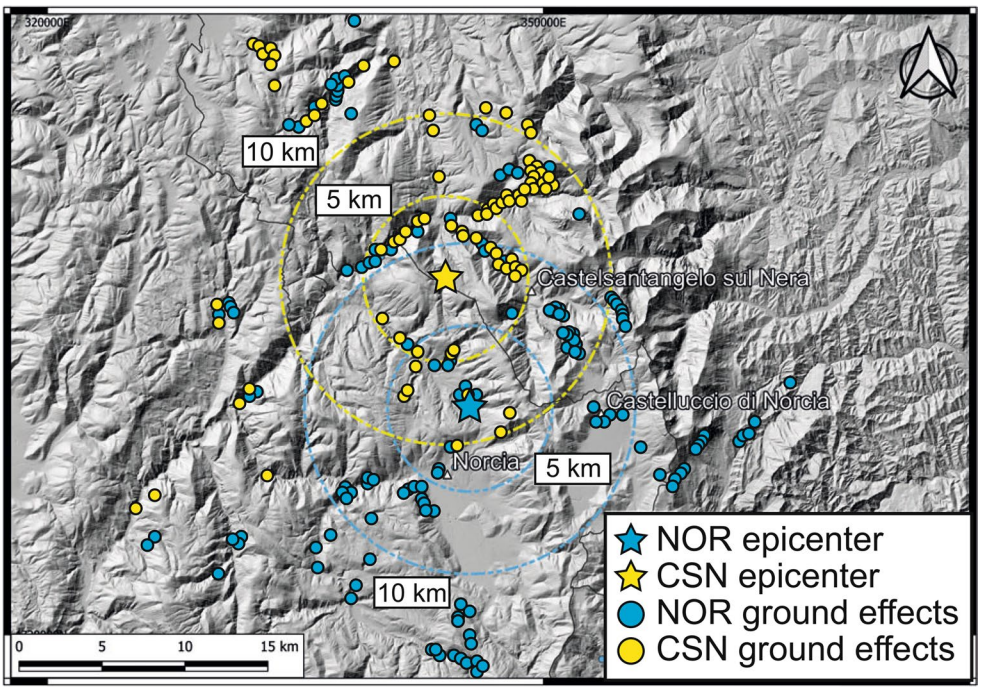

Fig. 10 Interference of effects between the CSN and NOR earthquakes referred to epicentral distances of 5 and 10 km, respectively

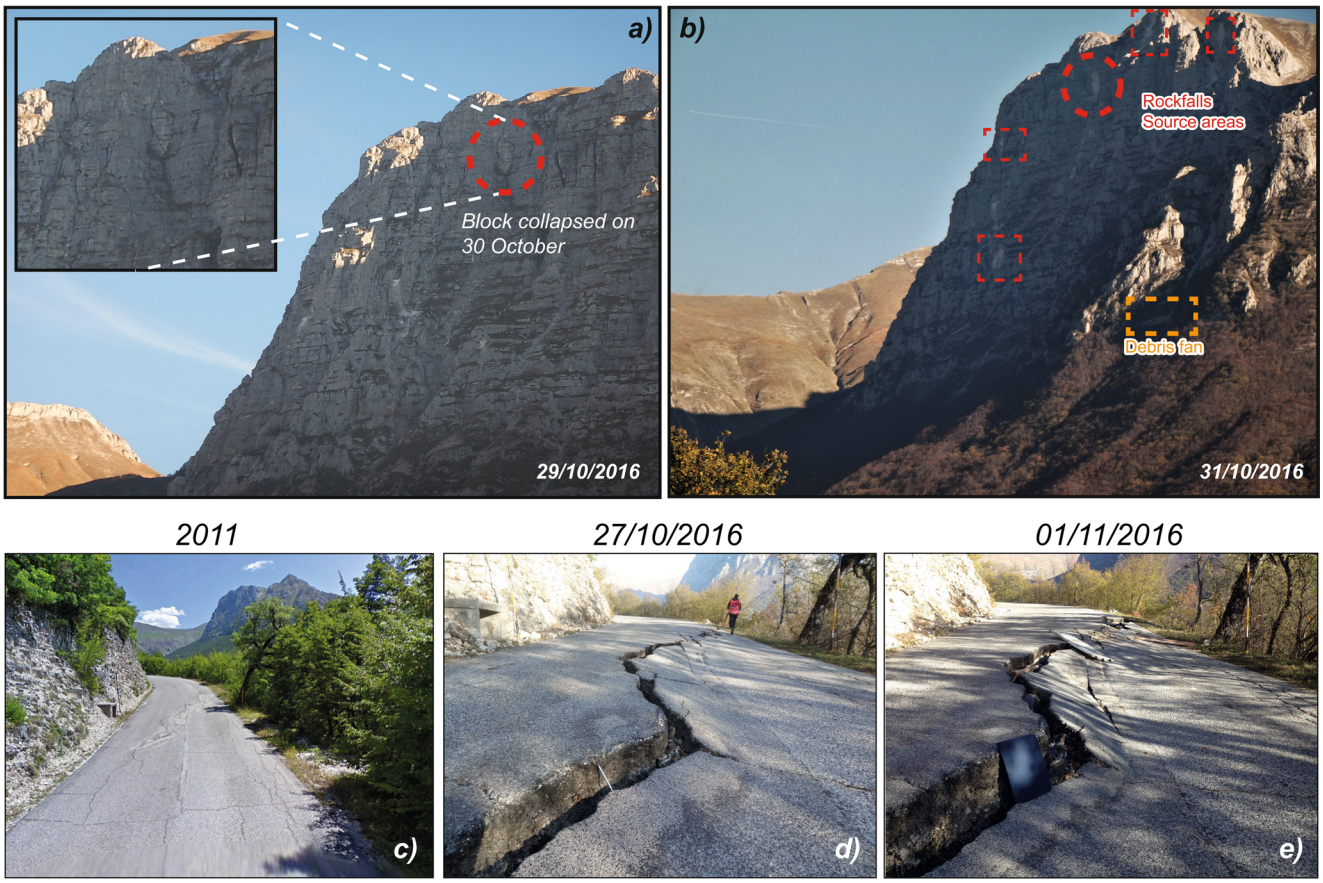

Fig. 11 **a**) Rock block detached from the northern cliff of Mt. Bove after the October 30, 2016, earthquake. The failure scar is visible in picture **b**. Subsequent reactivations of a coherent landslide in the municipality of Ussita (MC) were also surveyed following the main shocks of the CNS (Mw 5.8) on October 26, 2016 (**d**), and the NOR (Mw 6.5) on October 30, 2016 (**e**). These reactivations were observed on the dates corresponding to the surveys. The landslide impacted a local road that had already exhibited ground movement, as evidenced by circular-shaped ground cracks on the Google Street View image (**c**)

Discussion

The CEDIT catalogue is an open-access database supporting studies and research on earthquake-induced ground effects. It is a constantly updated inventory at the Italian national scale. This is a particularly relevant issue, considering that the CEDIT includes document-based evidence of effects on the ground, both historical and recent.

To discuss the completeness of the CEDIT catalogue, landslides are adopted here as a practical benchmark because they allow comparison with established reference frameworks and published datasets, whereas analogous quantitative benchmarks are less consistently available for other ground effects. The overall catalogue, however, systematically includes multiple classes of earthquake-induced ground effects.

Based on the last CEDIT release, it has been possible to develop and refine a national-level curve for the maximum expected distance of earthquake-induced disrupted landslide (*sensu* Keefer 1984), previously released by Martino et al. (2014). The Italian curve deviates from the global upper bound curve initially proposed by Keefer in 1984 and later updated by Rodriguez et al. in (1999). Given the magnitude of a seismic event, this curve allows for semi-empirical, highly reliable estimates of the extent of areas likely to be affected by earthquake-induced landslides (Martino et al. 2019). In the CEDIT updated version (Fig. 12), the curve deviates from the one previously proposed by Martino et al. (2014), particularly at lower magnitudes due to the occurrence of low-magnitude earthquakes that triggered disrupted landslides, such as the 2017 Ischia earthquake (Mw 3.9) and the 2019 Balsorano earthquake (Mw 4.6). At high magnitudes, the small mismatch between the Keefer curve and the Italian best-fit can instead be attributable to the fact that the Italian record includes fewer events to constrain the upper tail of maximum distances.

The CEDIT catalogue not only represents an inventory of documentary data, as intended to preserve the historical memory of past events, but it also aims to serve in the present as an effective training and validation dataset for quantitative analyses of earthquake-induced ground effect

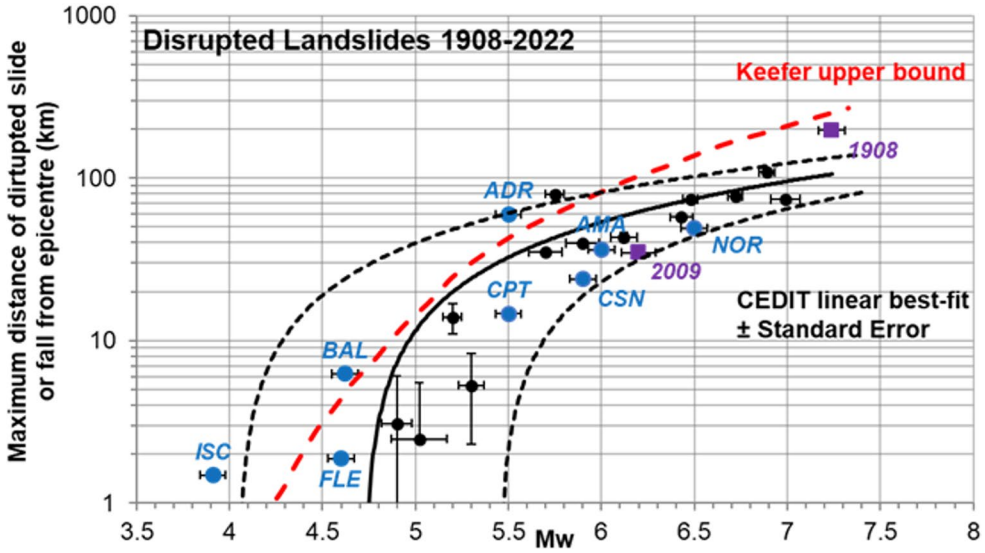

Fig. 12 Magnitude–distance relationships for disrupted landslides provided for Italian territory (black line), considering the main earthquakes from 1908 to 2025. The red dashed line represents the Keefer (1984) upper-bound curve for disrupted landslides (slide and rock fall), updated by Rodriguez et al. (1999). Black dashed lines refer to the standard error that straddles the CEDIT linear best-fit line (black line). In this version of the CEDIT-derived curve related to the 2025 release the earthquakes that occurred after 2012 are highlighted with respect the previous version dated back to 2014 (blue dots: AMA 2016, August 24th; CSN 2016, October 26th; NOR 2016, October 30th; Capitignano – CPT – 2017, January 18th; Ischia Island – ISC – 2017, August 21 st; Balsorano – BAL – 2019, November 07th; Adriatic Coast – ADR – 2022, November 09th; Campi Flegrei – FLE – 2025, June 30th) together with the earthquakes for which the catalogue has been updated, resulting in a change in the maximum epicentral distance of the induced effects (violet dots: 2009 L'Aquila and 1908 Reggio and Messina earthquakes). The black dots indicate the earthquakes that occurred in Italy before 2012, with which the first version of this curve, present in Martino et al. (2014), was constructed. Horizontal and vertical error bars represent event-level uncertainty affecting magnitude/source parameters and maximum-distance estimates, respectively. The dashed envelope around the best-fit curve represents the dispersion of the empirical constraint (standard deviation) and should be interpreted as an uncertainty band for scenario delineation based on the Italy-calibrated dataset

scenarios. Such products, considered as a physical scenario of environmental damages due to the seismic shaking, have the main goal of developing technical-scientific products functional to the management and mitigation of multi-hazard risks (Martino 2017). In this sense, the CEDIT represents a tool for analysing the distribution of earthquake-induced effects, and to reveal the environmental susceptibility variation, thus pointing out different predisposing conditions, and deriving more complex causal relationships between interdependent triggering and preparatory factors, such as initial soil conditions caused by antecedent rainfall (e.g., Martino et al. 2020a, b). This result also highlights the significance of the CEDIT catalogue for analyses of forward scenarios involving multiple independent causative factors.

However, the limited number of samples restricts further statistical analyses at a national scale. In this sense, and focusing on the earthquake-induced landslides, the concept of completeness that a landslide inventory must adhere to has been introduced and extensively discussed in the literature for its application to landslide hazard studies. Landslide datasets are frequently based on scattered data because the full spatial coverage is not entirely achievable. Malamud et al. (2004) highlight the importance of including a broad range of landslide sizes, particularly smaller ones, to ensure the completeness of landslide datasets. Tanyas and Lombardo (2020), and references therein, further refine this concept, defining completeness through the rollover point in landslide frequency-area plots, the extent of the landslide-affected area, and landslide susceptibility zones. Empirical curves designed to evaluate the frequency-size distribution of partial inventories, which were later refined by Tanyas et al. (2018) for earthquake-induced landslide datasets. These refinements enhance reliability, particularly when datasets include numerous small-scale landslides, enabling realistic estimates of power-law coefficients. Due to the historical nature, the presence of an archive-based dataset and the adopted inventorying and mapping criteria, CEDIT may not fully meet the completeness standard outlined in the literature. The earthquake-induced landslides in CEDIT are, in fact, represented as points rather than polygons, limiting the ability to estimate the areal or volumetric extent of landslides, except for recent ones. Despite this, the informative value from past earthquakes remains a crucial feature to be accounted for. CEDIT collects a significant amount of information regarding small-scale earthquake-induced landslides, which have been catalogued in recent times with the highest reliability regarding their location. This characteristic allows CEDIT to align with the completeness standards.

The availability of a landslide dataset densely populated with small-scale effects is ensured by on-site surveys, while such effects are often not identified by remote sensing techniques, which are increasingly being used to construct landslide datasets, usually bypassing detailed ground surveys entirely (Xu et al. 2014a, b, 2015; Martha et al. 2017; Tang et al. 2016; Hu et al. 2019; Karakas et al. 2021). It is also important to emphasise that small landslides are not less significant than larger ones, particularly when considering their role in scenario formulation and their impact on infrastructural assets. Small-scale landslides can have a substantial impact on road accessibility and emergency response efforts, making their inclusion in hazard assessments critical for developing more comprehensive and realistic scenarios.

The definition of the quality of a whole database must face off with the event inventory consistency, whose characteristics can present different completeness and accuracy. In general, the number of effects inventoried in the CEDIT, which is associated with a single earthquake, is higher for the most recent seismic events, since field surveying has been performed in the field. On the contrary, in the case of historical earthquakes, the identification of induced ground effects is indirect as it mainly relies on document-based sources (see Figs. 5 and 7). Additionally, the effects induced by lower-magnitude earthquakes may not have been included in the inventories as they were rarely reported in the chronicles or artworks.

Similar considerations can be assumed for the geolocation accuracy, which reaches its maximum value for recent earthquake-induced effects, thanks to the use of GPS during on-site surveys. Conversely, for earthquake-induced ground effects inventories from historical earthquakes included in the CEDIT catalogue, completeness depends on the availability of documentary sources and is characterised by a low degree of geolocation accuracy, typically ranging from Q1 to Q2, which mostly refers to the main municipality or general localities (Fig. 13).

For both recent and historical inventoried effects, there is a noticeable increase in the number as the magnitude of the seismic event increases. However, the rate of this increase varies between past and recent earthquakes (see Fig. 7). Despite absolute numbers, the coverage completeness of the CEDIT catalogue can be supported by the number of localities affected by earthquake-induced effects, normalised by the number of localities within the respective Keefer (1984) expected distance. This ratio shows a linear increase as the earthquake magnitude rises, with a trend that well represents both historical and recent events. This indicates that the catalogue consistently represents the earthquake coverage and impact on affected localities, i.e., those that had an MCS attribution in past events.

Inventories of ground effects induced by historical earthquakes are composed of an abundance of effects which depend on the availability of documentary sources. These effects are characterised by a low degree of location accuracy. At the same time, these types of historical inventories are useful for national-scale scenario analyses, for which a high accuracy in location is not prominent (Fig. 13).

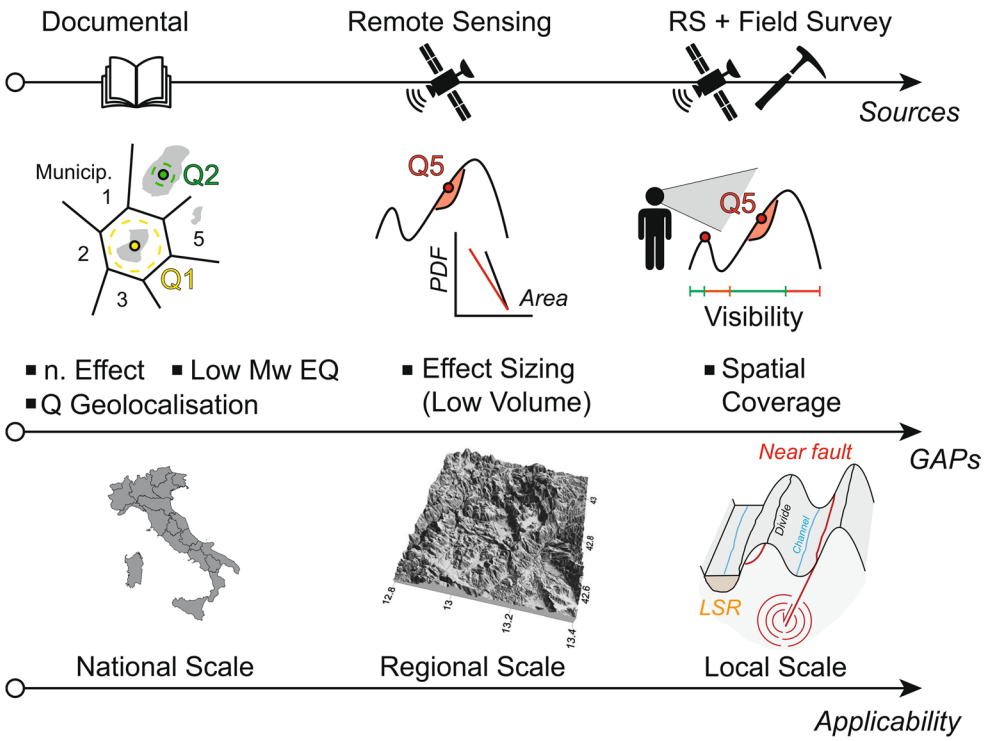

Fig. 13 Sketch representing the issues regarding the completeness and possible applications of catalogues of ground effects composed of data derived from documentary sources only (i.e., historical catalogues; left vertical), from remote sensing only (i.e., recent catalogue only; central vertical), from remote sensing and direct site surveying (i.e., both historical and recent catalogue; right vertical)

Moreover, the interest in reporting earthquake-induced ground effects in historical texts and chronicles was often limited to high-intensity effects, excluding those that did not interfere with human activities.

When referring to the inventories of effects induced by recent earthquakes, these are detected remotely or, in the best case, through direct ground surveys. If an inventory is based solely on remotely sensed data, it will usually have a high degree of geolocation accuracy, but the inventory may have gaps regarding small-scale effects, which cannot be detected remotely due to low resolution (Guzzetti et al. 2012; Xu et al. 2014b; Zhao 2021). For this reason, inventories composed solely of remotely sensed effects can be considered useful for regional-scale scenario analyses only and are limited for analysis of emergency conditions and impact on lifelines.

Even in the case of a direct survey, spatial completeness can be compromised by areas where there is no landscape visibility or post-earthquake accessibility. However, this issue does not undermine the usability of such inventories for detailed scenario analyses, which account for the local morphology, topographic amplification of seismic motion, near-fault effects, or geostructural factors.

Figure 13 conceptualises that different levels of completeness and accuracy can be managed in view of single inventory usage for susceptibility analysis and/or forward scenarios at several dimensional scales. In such a perspective, the entire CEDIT catalogue can be considered a tool for validating scenarios resulting from the application of data-driven artificial neural network approaches at a national scale, trained on both historical and recent ground effects (Amato et al. 2023).

It is therefore evident that for CEDIT-like catalogues, which compile data derived from the sum of individual inventories of ground effects induced by every recorded earthquake, it is appropriate to refer to two levels of completeness: (i) pertaining to the entire catalogue and (ii) one to the individual inventories (i.e., earthquake-specific) of effects that constitute it. Currently, the more thorough inventories that make up earthquake-induced ground effects catalogues are less historicised and, hence, less comprehensive from a temporal perspective. Therefore, regarding the catalogues (and not the individual inventories that compose them), it can be stated that completeness and historicity are complementary. In this sense, catalogues composed of only recent inventories have greater spatial completeness but less temporal coverage and, therefore, are less useful for scenario analyses that cover all possible spatial scales than temporal scales (i.e., not offering the possibility to conduct recurrence analyses). In the literature, it is possible to come across very detailed inventories of effects induced on the ground by earthquakes referring to single earthquakes that are considered complete for that earthquake but that, however, do not maintain the same level of completeness in the corresponding historical catalogues or those referring to multiple seismic events (Xu et al. 2014b; Roback et al. 2018).

To sum up this concept, we can state that nowadays the completeness of the CEDIT catalogue is affected by several factors, which include: (i) partial inventories of ground effects of both recent surveys and historical sources; (ii) potential interference among earthquakes which occurred in seismic sequences; (iii) limited information about low magnitude earthquakes due to their limited potential in inducing instabilities or to the scarce news about it in historical chronicles.

On the other hand, CEDIT's strength lies in being a densely populated catalogue of earthquake-induced ground effects, spanning a very large historical period, and representing a wide spatial distribution of effects, thus lending itself to various applications regarding susceptibility and scenario analyses in a territory with multiple seismogenic sources and a long time spanned documental record.

Conclusions

The most updated release of the CEDIT catalogue represents a significant update, incorporating ground effects from the 2016–2017 Central Italy seismic sequence, the 2022 Mw 5.5 earthquake, which caused landslides along the Adriatic coast, and other secondary seismic events. As a result, the CEDIT can be considered the most up-to-date catalogue of earthquake-induced ground effects available in Italy, offering comprehensive coverage of both historical and recent seismic events. The outcomes listed in the following offer a view of salient features in the last CEDIT release:

- Upgrade of the Italian earthquake magnitude vs. distance curve for disrupted landslides: the national curve for the maximum expected distance of earthquake-induced disrupted landslides (Martino et al. 2014), has been refined. This curve, coming from a linear best-fit, significantly different from the global upper bound curve (Keefer 1984), offers reliable semi-empirical estimates for landslide-affected epicentral distance based on earthquake magnitude, validated by the 2016–2017 Central Italy seismic sequence.
- Refining of the location accuracy: CEDIT excels in location accuracy for recent earthquake-induced ground effects due to the use of GPS in field surveys. In contrast, historical data relies on documentary sources, leading to variations in precision, especially for smaller-scale events.

- Check on dataset completeness: the completeness of the CEDIT entire catalogue is influenced by factors such as partial inventories, especially for historical earthquakes, and the limited information on smaller magnitude events. However, the detailed documentation of small-scale effects, especially recent ones, ensures alignment with completeness standards in landslide datasets.
- Filling of the historical earthquake data gaps: The completeness of historical inventories is limited by gaps in documentation, with small-scale events often missing from chronicles. The catalogue reflects these limitations, though recent data from direct field surveys provide a complete and more accurate picture of ground effects.
- Field-surveying contribution to the inventory: Small-scale landslides, often overlooked by remote sensing techniques, are crucial in scenario analyses, particularly in terms of their impact on accessibility and emergency response efforts. The inclusion of these events in the CEDIT dataset, thanks to the field surveys conducted in recent times after earthquakes, enhances the realism of hazard assessments and makes the inventories feasible for the depiction of future scenarios.

In general, the CEDIT catalogue represents a useful tool for multi-hazard analysis as it constitutes a historical archive that can be used to validate quantitative forward scenarios of earthquake-induced effects. This provides useful support for multi-hazard management and for direct strategies for hazard mitigation and resilience planning. In particular, CEDIT can be used as a quality-aware training and validation dataset for earthquake-induced landslide susceptibility at national-to-regional scales. In this sense, the workflow to be adopted includes (i) filtering records by effect type and location-quality class, (ii) delineating event footprints and comparing them with terrain variables and shaking proxies, and (iii) benchmarking susceptibility outputs against observed distributions across multiple events. For scenario modelling, the updated Italy-calibrated magnitude–maximum distance relationship for disrupted landslides provides an empirically constrained first-order extent for rapid screening; uncertainty should be propagated using the pointwise error bars and the dispersion envelope. The inclusion of small, field-mapped effects further improves the realism of lifeline impact analyses (road accessibility, emergency response), which are often underestimated by inventories that rely solely on remote sensing.

The CEDIT catalogue can be considered nowadays a reliable technical tool that enables support efforts to manage earthquake-related risks on a national scale, not only in Italy but also for training, using statistically-based approaches (i.e., machine learning for artificial intelligence) and tools to be exported abroad. In particular, with a view to training approaches for the statistical analysis of databases aimed at reconstructing forecast scenarios of earthquake-induced effects, the CEDIT, in combination with other similar international catalogues, represents a highly functional and fully available tool, given its open access.

Acknowledgements The authors would like to thank the working group of CERI, Centre for Research on Prediction, Prevention and Mitigation of Geological Risks, which carried out a field survey of the ground effects induced by the Mw 5.5, 2022, Adriatic coastal earthquake, composed of Dr Benedetta Antonielli, Dr Patrizia Caprari, Dr Federico Feliziani. The authors also thank Prof Mirko Francioni of the University of Urbino Carlo Bo for supporting the field surveying in 2022 and Tecnostudi Ambiente S.r.l. for the technical assistance in developing the new WEB platform of CERI.

Author contributions MF, GMM and SM: conceptualisation. MF, GMM, FF: field surveys, data analysis, writing – original paper. SM: project administration, writing – review and editing. All authors have read and agreed to the published version of the manuscript.

Funding Open access funding provided by Università degli Studi di Roma La Sapienza within the CRUI-CARE Agreement. The study was carried out within the RETURN Extended Partnership and received funding from the European Union Next-Generation EU (National Recovery and Resilience Plan – NRRP, Mission 4, Component 2, Investment 1.3 – D.D. 1243 2/8/2022, PE0000005).

Declarations

Competing interests The authors declare that they have no conflict of interest.

References

Alfaro P, Delgado J, García-Tortosa FJ, Giner JJ, Lenti L, López-Casado C, Martino S, Scarascia Mugnozza G (2012) The role of near-field interaction between seismic waves and slope on the triggering of a rockslide at Lorca (SE Spain). Nat Hazards Earth Syst Sci 12(12):3631–3643. https://doi.org/10.5194/nhess-12-3631-2012

Amato G, Fiorucci M, Martino S, Lombardo L, Palombi L (2023) Earthquake-triggered landslide susceptibility in Italy by means of artificial neural network. Bull Eng Geol Environ 82(5):160. https://doi.org/10.1007/s10064-023-03163-x

Bird JF, Bommer JJ (2004) Earthquake losses due to ground failure. Eng Geol 75(2):147–179. https://doi.org/10.1016/j.enggeo.2004.05.006
Brunetti MT, Guzzetti F, Rossi M (2009) Probability distributions of landslide volumes. Nonlinear Process Geophys 16(2):179–188. https://doi.org/10.5194/npg-16-179-2009
Burrows K, Marc O, Andermann C (2023) Retrieval of Monsoon landslide timings with Sentinel-1 reveals the effects of earthquakes and extreme rainfall. Geophys Res Lett 50(16):e2023GL104720. https://doi.org/10.1029/2023GL104720
Caprari P, Della Seta M, Martino S, Fantini A, Fiorucci M, Priore T (2018) Upgrade of the CEDIT database of earthquake-induced ground effects in Italy. Ital J Eng Geol Environ 18(2):23–39. https://doi.org/10.4408/IJEGE.2018-02.O-02
Chen XL, Zhou Q, Ran H, Dong R (2012) Earthquake-triggered landslides in Southwest China. Nat Hazards Earth Syst Sci 12(2):351–363. https://doi.org/10.5194/nhess-12-351-2012
Chiodini G, Paonita A, Aiuppa A, Costa A, Caliro S, De Martino P, Acocella V, Vandemeulebrouck J (2016) Magmas near the critical degassing pressure drive volcanic unrest towards a critical state. Nat Commun 7(1):13712. https://doi.org/10.1038/ncomms13712
Clague JJ (2022) Paleo-landslides. Landslide hazards, risks, and disasters. Elsevier, pp 335–363
Comerci V, Vittori E, Blumetti AM, Brustia E, Di Manna P, Guerrieri L, Lucarini M, Serva L (2015) Environmental effects of the December 28, 1908, Southern Calabria–Messina (Southern Italy) earthquake. Nat Hazards 76:1849–1891. https://doi.org/10.1007/s11069-014-1573-x
Crozier MJ (1992) Determination of palaeoseismicity from landslides. In: International symposium on landslides, A.A. Balkema, Rotterdam, pp 1173–1180
D'Auria L, Giudicepietro F, Aquino I, Borriello G, Del Gaudio C, Lo Bascio D, Martini M, Ricciardi G, Ricciolino P, Ricco C (2011) Repeated fluid-transfer episodes as a mechanism for the recent dynamics of Campi Flegrei caldera (1989–2010). J Geophys Res. https://doi.org/10.1029/2010JB007837
Delgado J, Garrido J, López-Casado C, Martino S, Peláez JA (2011) On far field occurrence of seismically induced landslides. Eng Geol 123(3):204–213. https://doi.org/10.1016/j.enggeo.2011.08.002
Del Gaudio C, Aquino I, Ricciardi GP, Ricco C, Scandone R (2010) Unrest episodes at Campi Flegrei: A reconstruction of vertical ground movements during 1905–2009. J Volcanol Geotherm Res 195(1):48–56. https://doi.org/10.1016/j.jvolgeores.2010.05.014
DISS Working Group (2021) Database of Individual Seismogenic Sources (DISS), Version 3.3.0: A compilation of potential sources for earthquakes larger than M 5.5 in Italy and surrounding areas. Istituto Nazionale di Geofisica e Vulcanologia (INGV)
EMERGEO Working Group (2010) Evidence for surface rupture associated with the Mw 6.3 L'Aquila earthquake sequence of April 2009 (central Italy). Terra Nova 22(1):43–51. https://doi.org/10.1111/j.1365-3121.2009.00915.x
EMERGEO Working Group (2016) The 24 August 2016 Amatrice earthquake: Coseismic Effects. https://doi.org/10.5281/zenodo.61568
Famiani D, Cara F, Di Giulio G et al (2025) Seismic survey in an urban area: the activities of the EMERSITO INGV emergency group in Ancona (Italy) following the 2022 M w 5.5 Costa Marchigiana–Pesarese earthquake. Earth Syst Sci Data 17(5):2087–2112. https://doi.org/10.5194/essd-17-2087-2025
Fan X, Scaringi G, Korup O et al (2019) Earthquake-induced chains of geologic hazards: Patterns, mechanisms, and impacts. Rev Geophys 57(2):421–503. https://doi.org/10.1029/2018RG000626
Ferrario MF (2019) Landslides triggered by multiple earthquakes: insights from the 2018 Lombok (Indonesia) events. Nat Hazards 98(2):575–592. https://doi.org/10.1007/s11069-019-03718-w
Fortunato C, Martino S, Prestininzi A, Romeo RW (2012) New release of the Italian catalogue of earthquake-induced ground failures (CEDIT). Ital J Eng Geol Environ 2:63–74. https://doi.org/10.4408/IJEGE.2012-02.O-05
Fullin N, Fraccaroli M, Francioni M, Fabbri S, Ballaera A, Ciavola P, Ghirotti M (2024) Detection of cliff top erosion drivers through machine learning algorithms between Portonovo and Trave cliffs (Ancona, Italy). Remote Sens 16(14):2604. https://doi.org/10.3390/rs16142604
Galli P (2000) New empirical relationships between magnitude and distance for liquefaction. Tectonophysics 324(3):169–187. https://doi.org/10.1016/S0040-1951(00)00118-9
Galli P, Castenetto S, Peronace E (2017) The macroseismic intensity distribution of the 30 October 2016 earthquake in central Italy (Mw 6.6): seismotectonic implications. Tectonics 36(10):2179–2191. https://doi.org/10.1002/2017TC004583
Govi M (1977) Photo-interpretation and mapping of the landslides triggered by the Friuli earthquake (1976). Bull Int Assoc Eng Geol. https://doi.org/10.1007/BF02592650
Guidoboni E, Ferrari G, Mariotti D, Comastri A, Tarabusi G, Sgattoni G, Valensise G (2018) CFTI5Med, Catalogo dei Forti Terremoti in Italia (461 a.C.-1997) e nell'area Mediterranea (760 a.C.-1500). Istituto Nazionale di Geofisica e Vulcanologia (INGV) https://doi.org/10.6092/ingv.it-cfti5
Guidoboni E, Ferrari G, Tarabusi G, Sgattoni G, Comastri A, Mariotti D, Ciuccarelli C, Bianchi MG, Valensise G (2019) CFTI5Med, the new release of the catalogue of strong earthquakes in Italy and in the Mediterranean area. Sci Data 6(1):80. https://doi.org/10.1038/s41597-019-0091-9
Guzzetti F, Mondini AC, Cardinali M, Fiorucci F, Santangelo M, Chang KT (2012) Landslide inventory maps: new tools for an old problem. Earth-Sci Rev 112(1–2):42–66. https://doi.org/10.1016/j.earscirev.2012.02.001
Harp EL, Jibson RW (1995) Inventory of landslides triggered by the 1994 Northridge, California earthquake. US Geological Survey, pp 95–213
Harp EL, Jibson RW (1996) Landslides triggered by the 1994 Northridge, California, earthquake. Bull Seismol Soc Am 86(1B):S319–S332. https://doi.org/10.1785/BSSA08601BS319
Harp EL, Keefer DK (1990) 18. Landslides triggered by the earthquake. U S Geol Surv Prof Pap 1487:335
Harp EL, Keefer DK, Sato HP, Yagi H (2011) Landslide inventories: the essential part of seismic landslide hazard analyses. Eng Geol 122(1–2):9–21. https://doi.org/10.1016/j.enggeo.2010.06.013
Harp EL, Wilson RC, Wieczorek GF (1981) Landslides from the February 4, 1976, Guatemala earthquake (No. 1204). US Government Printing Office
Hofer L, Zampieri P, Zanini MA, Faleschini F, Pellegrino C (2018) Seismic damage survey and empirical fragility curves for churches after the August 24, 2016 Central Italy earthquake. Soil Dyn Earthq Eng 111:98–109. https://doi.org/10.1016/j.soildyn.2018.02.013
Hu K, Zhang X, You Y, Hu X, Liu W, Li Y (2019) Landslides and dammed lakes triggered by the 2017 Ms6. 9 Milin earthquake in the Tsangpo gorge. Landslides 16:993–1001. https://doi.org/10.1007/s10346-019-01168-w
Jibson RW (1996) Use of landslides for paleoseismic analysis. Eng Geol 43(4):291–323. https://doi.org/10.1016/S0013-7952(96)00039-7
Karakas G, Nefeslioglu HA, Kocaman S, Buyukdemircioglu M, Yurur T, Gokceoglu C (2021) Derivation of earthquake-induced landslide distribution using aerial photogrammetry: the January 24, 2020, Elazig (Turkey) earthquake. Landslides 18(6):2193–2209. https://doi.org/10.1007/s10346-021-01660-2
Keefer DK (1984) Landslides caused by earthquakes. Geol Soc Am Bull 95(4):406–421. https://doi.org/10.1130/0016-7606(1984)95%3C;406:LCBE%3E;2.0.CO;2
Keefer DK (2002) Investigating landslides caused by earthquakes - A historical review. Surv Geophys 23(6):473–510. https://doi.org/10.1023/A:1021274710840

Malamud BD, Turcotte DL, Guzzetti F, Reichenbach P (2004) Landslide inventories and their statistical properties. Earth Surf Process Landf 29(6):687–711. https://doi.org/10.1002/esp.1064

Marmoni GM, Martino S, Censi M, Menichetti M, Piacentini D, Scarascia Mugnozza G, Torre D, Troiani F (2023) Transition from rock mass creep to progressive failure for rockslide initiation at Mt. Conero (Italy). Geomorphology 437:108750. https://doi.org/10.1016/j.geomorph.2023.108750

Marques FMSF (2008) Magnitude-frequency of sea cliff instabilities. Nat Hazards Earth Syst Sci 8(5):1161–1171. https://doi.org/10.5194/nhess-8-1161-2008

Martha TR, Roy P, Mazumdar R, Govindharaj KB, Kumar KV (2017) Spatial characteristics of landslides triggered by the 2015 M w 7.8 (Gorkha) and M w 7.3 (Dolakha) earthquakes in Nepal. Landslides 14:697–704. https://doi.org/10.1007/s10346-016-0763-x

Martino S (2017) Eartquake-induced landslides in Italy. from the distribution of effects to the hazard mapping. Ital J Eng Geol Environ 1:53–67. https://doi.org/10.4408/IJEGE.2017-01.O-04

Martino S, Antonielli B, Bozzano F, Caprari P, Discenza ME, Esposito C, Fiorucci M, Iannucci R, Marmoni GM, Schilirò L (2020a) Landslides triggered after the 16 August 2018 M w 5.1 Molise earthquake (Italy) by a combination of intense rainfalls and seismic shaking. Landslides 17:1177–1190. https://doi.org/10.1007/s10346-020-01359-w

Martino S, Bozzano F, Caporossi P et al (2017) Ground effects triggered by the 24th August 2016, Mw 6.0 Amatrice (Italy) earthquake: surveys and inventorying to update the CEDIT catalogue. Geog Fis Din Quat 40(1):77–95. https://doi.org/10.4461/GFDQ.2017.40.7

Martino S, Bozzano F, Caporossi P et al (2019) Impact of landslides on transportation routes during the 2016–2017 Central Italy seismic sequence. Landslides 16:1221–1241. https://doi.org/10.1007/s10346-019-01162-2

Martino S, Caprari P, Fiorucci M, Marmoni GM (2020b) The CEDIT catalogue: from inventorying of earthquake-induced ground effects to analysis of scenario. Mem Descr Carta Geol d'Italia 107:441–452

Martino S, Fiorucci M, Marmoni GM, Casaburi L, Antonielli B, Mazzanti P (2022) Increase in landslide activity after a low-magnitude earthquake as inferred from DInSAR interferometry. Sci Rep 12(1):2686. https://doi.org/10.1038/s41598-022-06508-w

Martino S, Prestininzi A, Romeo RW (2014) Earthquake-induced ground failures in Italy from a reviewed database. Nat Hazards Earth Syst Sci 14(4):799–814. https://doi.org/10.5194/nhess-14-799-2014

Meletti C, Patacca E, Scandone P (2000) Construction of a seismotectonic model: the case of Italy. Pure Appl Geophys 157:11–35. https://doi.org/10.1007/978-3-0348-8415-0_2

Meunier P, Hovius N, Haines JA (2008) Topographic site effects and the location of earthquake induced landslides. Earth Planet Sci Lett 275(3–4):221–232. https://doi.org/10.1016/j.epsl.2008.07.020

Mikoš M, Jemec M, Ribičič M, Čarman M, Komac M (2013) Earthquake-induced landslides in Slovenia: historical evidence and present analyses. In Earthquake-Induced Landslides. In: Proceedings of the International Symposium on Earthquake-Induced Landslides, Kiryu, Japan, Springer Berlin Heidelberg, pp. 225–233

Locati M, Camassi R, Rovida A et al (2022) Database Macrosismico Italiano (DBMI15. https://doi.org/10.13127/dbmi/dbmi15.4. versione 4.0 [Data set]Istituto Nazionale di Geofisica e Vulcanologia (INGV)

Orsi G, De Vita S, Di Vito M (1996) The restless, resurgent Campi Flegrei nested caldera (Italy): constraints on its evolution and configuration. J Volcanol Geotherm Res 74(3–4):179–214. https://doi.org/10.1016/S0377-0273(96)00063-7

Papadopoulos GA, Plessa A (2000) Magnitude–distance relations for earthquake-induced landslides in Greece. Eng Geol 58(3–4):377–386. https://doi.org/10.1016/S0013-7952(00)00043-0

Petrosino S, Cusano P, Madonia P (2018) Tidal and hydrological periodicities of seismicity reveal new risk scenarios at Campi Flegrei caldera. Sci Rep 8(1):13808. https://doi.org/10.1038/s41598-018-31760-4

Petrosino S, Ricco C, De Lauro E, Aquino I, Falanga M (2020) Time evolution of medium and long-period ground tilting at Campi Flegrei caldera. Adv Geosci 52:9–17. https://doi.org/10.5194/adgeo-52-9-2020

Piacentini D, Troiani F, Torre D, Menichetti M (2021) Land-surface quantitative analysis to investigate the spatial distribution of gravitational landforms along rocky coasts. Remote Sens 13(24):5012. https://doi.org/10.3390/rs13245012

Pizza M, Ferrario F, Michetti AM, Velázquez-Bucio MM, Lacan P, Porfido S (2024) Intensity prediction equations based on the Environmental Seismic Intensity (ESI-07) Scale: application to normal fault earthquakes. Appl Sci 14(17):8048. https://doi.org/10.3390/app14178048

Prestininzi A, Romeo RW (2000) Earthquake-induced ground failures in Italy. Eng Geol 58(3–4):387–397. https://doi.org/10.1016/S0013-7952(00)00044-2

Pucci S, De Martini PM, Civico R et al (2017) Coseismic ruptures of the 24 August 2016, Mw 6.0 Amatrice earthquake (central Italy). Geophys Res Lett 44(5):2138–2147. https://doi.org/10.1002/2016GL071859

Rasanen RA, Maurer BW (2022) Probabilistic seismic source inversion from regional landslide evidence. Landslides 19(2):407–419. https://doi.org/10.1007/s10346-021-01780-9

Roback K, Clark MK, West AJ, Zekkos D, Li G, Gallen SF, Chamlagain D, Godt JW (2018) The size, distribution, and mobility of landslides caused by the 2015 Mw7. 8 Gorkha earthquake, Nepal. Geomorphology 301:121–138. https://doi.org/10.1016/j.geomorph.2017.01.030

Rodrıguez CE, Bommer JJ, Chandler RJ (1999) Earthquake-induced landslides: 1980–1997. Soil Dyn Earthq Eng 18(5):325–346. https://doi.org/10.1016/S0267-7261(99)00012-3

Romeo R, Delfino L (1997) CEDIT: Catalogo Nazionale degli effetti deformativi del suolo indotti da forti terremoti. Rapporto tecnico SSN/RT/97/04.

Rovida A, Locati M, Camassi R, Lolli B, Gasperini P (2020a) Catalogo Parametrico dei Terremoti Italiani (CPTI15), versione 2.0. Istituto Nazionale di Geofisica e Vulcanologia (INGV)

Rovida A, Locati M, Camassi R, Lolli B, Gasperini P (2020b) The Italian earthquake catalogue CPTI15. Bull Earthq Eng 18(7):2953–2984. https://doi.org/10.1007/s10518-020-00818-y

Sato HP, Harp EL (2009) Interpretation of earthquake-induced landslides triggered by the 12 May 2008, M7. 9 Wenchuan earthquake in the Beichuan area, Sichuan Province, China using satellite imagery and Google Earth. Landslides 6:153–159. https://doi.org/10.1007/s10346-009-0147-6

Sbarra P, Burrato P, Tosi P, Vannoli P, De Rubeis V, Valensise G (2019) Inferring the depth of pre-instrumental earthquakes from macroseismic intensity data: a case-history from Northern Italy. Sci Rep 9(1):15583. https://doi.org/10.1038/s41598-019-51966-4

Sepúlveda SA, Murphy W, Jibson RW, Petley DN (2005) Seismically induced rock slope failures resulting from topographic amplification of strong ground motions: the case of Pacoima Canyon. Calif Eng Geol 80(3–4):336–348. https://doi.org/10.1016/j.enggeo.2005.07.004

Sisti R, Di Ludovico M, Borri A, Prota A (2019) Damage assessment and the effectiveness of prevention: the response of ordinary unreinforced masonry buildings in Norcia during the Central Italy 2016–2017 seismic sequence. Bull Earthq Eng 17:5609–5629. https://doi.org/10.1007/s10518-018-0448-z

Stucchi M, Meletti C, Montaldo V, Crowley H, Calvi GM, Boschi E (2011) Seismic hazard assessment (2003–2009) for the Italian

building code. Bull Seismol Soc Am 101(4):1885–1911. https://doi.org/10.1785/0120100130

Tang C, Van Westen CJ, Tanyas H, Jetten VG (2016) Analysing post-earthquake landslide activity using multi-temporal landslide inventories near the epicentral area of the 2008 Wenchuan earthquake. Nat Hazards Earth Syst Sci 16(12):2641–2655. https://doi.org/10.5194/nhess-16-2641-2016

Tanyaş H, Allstadt KE, van Westen CJ (2018) An updated method for estimating landslide-event magnitude. Earth Surf Process Landf 43(9):1836–1847. https://doi.org/10.1002/esp.4359

Tanyaş H, van Westen CJ, Allstadt KE, Jessee ANM, Görüm T, Jibson RW, Godt JW, Sato HP, Schmitt RG, Odin M, Hovius N (2017) Presentation and analysis of a worldwide database of earthquake-induced landslide inventories. J Geophys Res Earth Surf 122(10):1991–2015. https://doi.org/10.1002/2017JF004236

Tanyaş H, van Westen CJ, Allstadt KE, Jibson RW (2019) Factors controlling landslide frequency–area distributions. Earth Surf Process Landf 44(4):900–917. https://doi.org/10.1002/esp.4543

Tanyas H, Lombardo L (2020) Completeness index for earthquake-induced landslide inventories. Eng Geol 264:105331. https://doi.org/10.1016/j.enggeo.2019.105331

Troiani F, Martino S, Marmoni GM, Menichetti M, Torre D, Iacobucci G, Piacentini D (2020) Integrated field surveying and land surface quantitative analysis to assess landslide proneness in the Conero Promontory rocky coast (Italy). Appl Sci Basel 10(14):4793. https://doi.org/10.3390/app10144793

Varnes DJ (1978a) Slope movement types and processes. Special Rep 176:11–33

Varnes DJ (1978b) Slope movement types and processes. Special report, 176. National Academy of Sciences and Transportation Research Board, pp. 11–33

Velázquez-Bucio MM, Ferrario MF, Lacan P et al (2024) Environmental effects and ESI-07 intensity of the Mw 7.7, September 19th, 2022, Michoacán, Mexico, earthquake. Eng Geol 343:107776. https://doi.org/10.1016/j.enggeo.2024.107776

Villani F, Civico R, Pucci S, Pizzimenti L, Nappi R, De Martini PM (2018) A database of the coseismic effects following the 30 October 2016 Norcia earthquake in Central Italy. Sci Data 5(1):1–11. https://doi.org/10.1038/sdata.2018.49

Vitale S, Isaia R (2014) Fractures and faults in volcanic rocks (Campi Flegrei, Southern Italy): insight into volcano-tectonic processes. Int J Earth Sci 103(3):801–819. https://doi.org/10.1007/s00531-013-0979-0

Wasowski J, Keefer DK, Lee CT (2011) Toward the next generation of research on earthquake-induced landslides: current issues and future challenges. Eng Geol 122(1–2):1–8. https://doi.org/10.1016/j.enggeo.2011.06.001

Wills CJ, McCrink TP (2002) Comparing landslide inventories: the map depends on the method. Environ Eng Geosci 8(4):279–293. https://doi.org/10.2113/8.4.279

Xu C, Xu X, Shyu JBH (2015) Database and spatial distribution of landslides triggered by the Lushan, China Mw 6.6 earthquake of 20 April 2013. Geomorphology 248:77–92. https://doi.org/10.1016/j.geomorph.2015.07.002

Xu C, Xu X, Shyu JBH, Zheng W, Min W (2014a) Landslides triggered by the 22 July 2013 Minxian–Zhangxian, China, Mw 5.9 earthquake: inventory compiling and spatial distribution analysis. J Asian Earth Sci 92:125–142. https://doi.org/10.1016/j.jseaes.2014a.06.014

Xu C, Xu X, Yao X, Dai F (2014b) Three (nearly) complete inventories of landslides triggered by the May 12, 2008 Wenchuan Mw 7.9 earthquake of China and their spatial distribution statistical analysis. Landslides 11:441–461. https://doi.org/10.1007/s10346-013-0404-6

Yagi H, Sato G, Higaki D, Yamamoto M, Yamasaki T (2009) Distribution and characteristics of landslides induced by the Iwate–Miyagi Nairiku Earthquake in 2008 in Tohoku District, Northeast Japan. Landslides 6:335–344. https://doi.org/10.1007/s10346-009-0182-3

Zei C, Tarabusi G, Ciuccarelli C, Burrato P, Sgattoni G, Taccone RC, Mariotti D (2024a) CFTIlandslides, Italian database of historical earthquake-induced landslides. Sci Data 11(1):834. https://doi.org/10.1038/s41597-024-03692-4

Zei C, Tarabusi G, Ciuccarelli C, Burrato P, Sgattoni G, Taccone RC, Mariotti D (2024b) CFTIlandslides, Italian database of historical earthquake-induced landslides. Istituto Naz di Geofis e Vulcanologia (INGV). https://doi.org/10.13127/cfti/landslides

Zhao B (2021) Landslides triggered by the 2018 Mw 7.5 Palu supershear earthquake in Indonesia. Eng Geol 294:106406. https://doi.org/10.1016/j.enggeo.2021.106406